The influence of size and charge of chitosan/ polyglutamic acid hollow spheres on cellular internalization, viability and blood compatibility

Elsevier Editorial System(tm) for Biomaterials
Manuscript Draft

Manuscript Number:

Title: Tunable chitosan/polyglutamic acid hollow spheres: A model system to study size and charge effect on cellular internalization, viability and blood compatibility

Article Type: FLA Original Research

Section/Category: Biomaterials & Nanotechnology

Keywords: size, surface charge, cell viability, internalization, blood compatibility, nanospheres, microspheres

Corresponding Author: Dr. Abhay Pandit,

Corresponding Author's Institution: National University of Ireland

First Author: Biraja C Dash, MS

Order of Authors: Biraja C Dash, MS; Gildas Rethore, PhD; Michael Monaghan, BE; Kathleen Fitzgerald, PhD; William Gallagher, PhD; Abhay Pandit

Abstract: Polymeric hollow spheres because of their tunable properties can be used as efficient carriers of various therapeutic molecules. However, the entry of these synthetic vehicles into cells, their cell viability and blood compatibility depend on their physical and chemical properties e.g. size, surface charge. Herein, we report the effect of size and surface charge on cell viability and cellular internalization behaviour and their effect on various blood components using chitosan/polyglutamic acid hollow spheres as a model system. Negatively charged chitosan/polyglutamic acid hollow spheres of various sizes 100, 300, 500 and 1000nm were fabricated using a template based method and covalently surface modified using linear polyethylene glycol and methoxyethanol amine to create a gradient of surface charge from negative to neutrally charged spheres respectively. The results here suggest that both size and surface charge have a significant influence on the sphere's behaviour, most prominently on haemolysis, platelet activation, plasma recalcification time, cell viability and internalization over time. Additionally, cellular internalization behaviour and viability was found to vary with different cell types. These results are in agreement with those of inorganic spheres and liposomes, and can serve as guidelines for tailoring polymeric solid spheres for specific desired applications in biological and pharmaceutical fields, including the design of nano to submicron sized delivery vehicles.

MANDATORY AUTHOR DECLARATION

An Author Declaration is a mandatory part of a submission. This Declaration covers a number of logistic and ethical issues which are described below. A template for the covering letter will be found at the end of this document. Authors may save this template, obtain the required signatures and then upload it as a part of their submission.

Corresponding Author

The name, address, and valid email address of the corresponding author. The Corresponding Author is the person who is responsible for the manuscript as it moves through the journal's submission process. This person must be registered with Editorial Manager as all correspondence pertaining to the manuscript will be sent to him/her via the system. *The Corresponding Author is the person responsible for making any edits/submitting revisions to the manuscript and is the only author who may view the progress of the manuscript as it moves from one stage to the next. He/she is responsible for communicating with the other authors about progress, revisions and final approval of the proofs and is the only authorised contact with the Editorial Office.*

Redundant or Duplicate Publication

Redundant or duplicate publication is publication of a paper that overlaps substantially with one already published. If redundant or duplicate publication is attempted or occurs without notification to the Editor, authors should expect editorial action to be taken.

When submitting a paper, the author should always make a full statement to the editor about all submissions and previous papers that might be regarded as redundant or duplicate publication of the same or very similar work. The author should alert the editor if the work includes subjects about which a previous paper has been published. Any such work should be referred to and referenced in the new paper. Copies of such material, including papers in press, should be included with the submitted paper to assist the editor in determining how to handle the matter.

Authorship

It is required that the Author Declaration be signed by all authors. All persons designated as authors should qualify for authorship, and all those who qualify should be listed. Each author should have participated sufficiently in the work to take public responsibility for appropriate portions of the content. The corresponding author should take responsibility for the integrity of the work as a whole, from inception to published article.
Authorship credit should be based only on 1) substantial contributions to conception and design, or acquisition of data, or analysis and interpretation of data; 2) drafting the article or revising it critically for important intellectual content; and 3) final approval of the version to be published. Conditions 1, 2, and 3 must all be met.

The order of authorship on the by-line is a matter for the institution(s) and must be agreed by all named authors prior to submission.

Conflict of Interest

Author conflict of interest for a given manuscript exists when an author has ties to activities that could inappropriately influence his or her judgment, whether or not judgment is in fact affected. Financial relationships with industry are usually considered to be the most important conflicts of interest.

When submitting a manuscript authors are responsible for recognizing and disclosing financial and other conflicts of interest that might bias their work. They should acknowledge in the manuscript all financial support for the work and other financial or personal connections to the work. If there are no such conflicts or financial support to acknowledge, the authors should declare this by the following statement: *The authors confirm that there are*

MANDATORY AUTHOR DECLARATION

no known conflicts of interest associated with this publication and there has been no significant financial support for this work that could have influenced its outcome.

Ethical Issues

When reporting experiments on animals, authors should indicate whether the institution's or a national research council's guide for, or any national law on, the care and use of laboratory animals was followed. When reporting experiments on human subjects, authors should indicate whether the procedures followed were in accordance with the ethical standards of the responsible committee on human experimentation (institutional or regional) and with the Helsinki Declaration of 1975, as revised in 1983.

This means that the authors must make a clear statement that the laws which apply to them in their own country were followed. This is best done as a statement under the section Materials & Methods.

Acknowledgements

All contributors who do not meet the criteria for authorship, such as a person who provided purely technical help, writing assistance, or a department chair who provided only general support should be listed in the acknowledgments. Financial and material support should also be recognised in the acknowledgments.

Impact Statement

Authors are encouraged to include in their covering letter a statement of their understanding of the importance and impact of their work. This should not be speculation on vague possibilities for clinical use but a precise statement relating to the underlying science. A concise statement of this impact should be included at the end of the Abstract.

AUTHOR DECLARATION TEMPLATE

We the undersigned declare that this manuscript is original, has not been published before and is not currently being considered for publication elsewhere.

We wish to draw the attention of the Editor to the following facts which may be considered as potential conflicts of interest and to significant financial contributions to this work. [OR]
We wish to confirm that there are no known conflicts of interest associated with this publication and there has been no significant financial support for this work that could have influenced its outcome.

We confirm that the manuscript has been read and approved by all named authors and that there are no other persons who satisfied the criteria for authorship but are not listed. We further confirm that the order of authors listed in the manuscript has been approved by all of us.

We confirm that we have given due consideration to the protection of intellectual property associated with this work and that there are no impediments to publication, including the timing of publication, with respect to intellectual property. In so doing we confirm that we have followed the regulations of our institutions concerning intellectual property.

We understand that the Corresponding Author is the sole contact for the Editorial process (including Editorial Manager and direct communications with the office). He/she is responsible for communicating with the other authors about progress, submissions of revisions and final approval of proofs. We confirm that we have provided a current, correct email address which is accessible by the Corresponding Author and which has been configured to accept email from biomaterials@online.be.

Signed by all authors as follows:

Biraja C. Dash 

Gildas Rethore 

Michael Monaghan 

Kathleen Fitzgerald 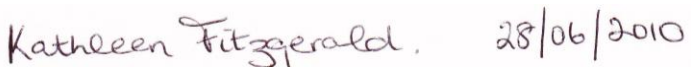

William Gallaghar 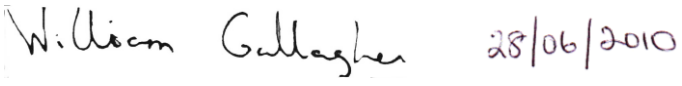

Abhay Pandit 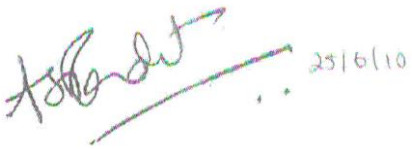

Network of Excellence for Functional Biomaterials
National University of Ireland, Galway
Telephone: +353 (0) 91 495833
Fax: +353 (0) 91 495585
Email: nfb@nuigalway.ie

30th June 2010

Dear David

It is our pleasure to submit the manuscript entitled *'Tunable chitosan/polyglutamic acid hollow spheres: A model system to study size and charge effect on cellular internalization, viability and blood compatibility'* for consideration for publication in *Biomaterials*. We feel that this manuscript is particularly significant for a number of reasons. It presents a model system for producing hollow spheres with tunable structural characteristics, namely size and surface chemistry. This is the first study to our knowledge that reports the combinatorial effect of two parameters (size and surface modifications) of these hollow spheres on blood components, cellular internalization and cell viability. We believe that the model system and parameters presented in this manuscript can be of potential value to serve as guidelines for predicting behaviour of spheres for specific desired applications in the drug delivery field, including design of nano to submicron sized delivery vehicles.

Our previous work in this area has been published in the following journals:

- Rethore G, Mathew A, Naik H, Pandit A. Preparation of chitosan/polyglutamic acid spheres based on the use of polystyrene template as a nonviral gene carrier. Tissue Eng Part C Methods 2009; 15(4): 605-13.

Network of Excellence for Functional Biomaterials
National University of Ireland, Galway
Telephone: +353 (0) 91 495833
Fax: +353 (0) 91 495585
Email: nfb@nuigalway.ie

- Rethore G, Pandit A. Use of templates to fabricate nanoscale spherical structures for defined architectural control. Small 2010; 6(4): 488-98.

We look forward to hearing from you with regard to the status of this manuscript and welcome your esteemed comments.

Sincerely

Abhay Pandit

*Title Page

Tunable chitosan/polyglutamic acid hollow spheres: A model system to study size and charge effect on cellular internalization, viability and blood compatibility

Biraja C. Dash[1#], Gildas Réthoré[1#], Michael Monaghan[1], Kathleen Fitzgerald[2], William Gallagher[2], Abhay Pandit[1]*

1 - Network of Excellence for Functional Biomaterials, National University of Ireland Galway, Galway, Ireland

2 - UCD School of Biomolecular and Biomedical Science, University College Dublin, Dublin, Ireland

# Authors contributed equally

* To whom Correspondence should be addressed

Abhay Pandit

Postal Address: Network of Excellence for Functional Biomaterials (NFB)
IDA Business Park, Dangan,
National University of Ireland Galway,
Galway,
Ireland

Telephone: +353-91-49 2758

Email: abhay.pandit@nuigalway.ie

Short title: Tunable Chitosan/Polyglutamic Acid Hollow Spheres

Abstract

Polymeric hollow spheres because of their tunable properties can be used as efficient carriers of various therapeutic molecules. However, the entry of these synthetic vehicles into cells, their cell viability and blood compatibility depend on their physical and chemical properties e.g. size, surface charge. Herein, we report the effect of size and surface charge on cell viability and cellular internalization behaviour and their effect on various blood components using chitosan/polyglutamic acid hollow spheres as a model system. Negatively charged chitosan/polyglutamic acid hollow spheres of various sizes 100, 300, 500 and 1000nm were fabricated using a template based method and covalently surface modified using linear polyethylene glycol and methoxyethanol amine to create a gradient of surface charge from negative to neutrally charged spheres respectively. The results here suggest that both size and surface charge have a significant influence on the sphere's behaviour, most prominently on haemolysis, platelet activation, plasma recalcification time, cell viability and internalization over time. Additionally, cellular internalization behaviour and viability was found to vary with different cell types. These results are in agreement with those of inorganic spheres and liposomes, and can serve as guidelines for tailoring polymeric solid spheres for specific desired applications in biological and pharmaceutical fields, including the design of nano to submicron sized delivery vehicles.

Keywords: size, surface charge, cell viability, internalization, blood compatibility, nanospheres, microspheres

1. Introduction

Nanoscale technology, an emerging field in biomaterials offers the opportunity of developing and optimizing biomaterials in a clinically translational form such as synthetic capsules or hollow spheres to deliver therapeutics [1]. In the past few decade there has been growing interest in the design of biomaterial-based delivery vehicles to use them as a depot for various therapeutic molecules *e.g.* gene, growth factors [1-6]. Among several methods for the fabrication of hollow spherical structures from synthetic or natural polymer, the template based method is an attractive in creating monodisperse nano to micron-sized hollow spheres [7]. The template method employs either coating of a single polymer or layer by layer coating of multiple polymers on a sacrificial template [4, 8]. Hollow spheres thus fabricated can be designed with various structural characteristics such as surface charge, size, shell thickness, pore size and mechanical strength. These modifications allow for efficient loading and sustained release of various therapeutics e.g. genes, peptides and drugs for the desired clinical targets [7].

However, therapeutic efficacy of any micro or nano size delivery vehicle depends on their cellular internalization behaviour, cell viability and blood compatibility. It is now an established fact that small physicochemical differences have significant biological implications in the cellular internalization and other biological processes of solid spheres [9]. Size and surface charge can affect the efficiency and pathway of cellular internalization for liposomes [10], quantum dots [11], polymeric spheres [12, 13], gold spheres [14, 15], silver [15] and silica spheres [16] by influencing the adhesion of the particles and their interaction with cells [17]. Also, for in vitro cytotoxicity and haemotoxicity studies, the careful and accurate characterization of particle size, surface charge is crucial issues [18-24]. Thus *in vitro* experimental studies with consistency of sphere size and surface charge are desired for elucidating the effects of these properties on cellular internalization, viability and blood compatibility.

Previous investigations on the effects of sphere size and surface charge offered modest consideration to independently alter one variable at a time while monitoring the effect of each variable [16, 24, 25]. Although commercially available fluorescent polystyrene (PS) beads have been used as a model and extensively applied in evaluating the effect of particle size on cellular internalization and blood compatibility behaviour [12, 13, 24, 26, 27, 28] the difficulties in controlling the surface charge during the size control processes and the lack in surface functionality impaired the precise evaluation of the relationship between physicochemical properties of polymeric spheres and their biological process [12, 27]. No study to date has reported on the combinatorial effect of studies of size and charge.

Herein, it was hypothesized that polymeric hollow sphere prepared using a template based method can be used as a model system to study combinatorial effect of surface charge and size on cell viability, cellular uptake and blood compatibility. The specific objectives of this study were to fabricate monodisperse chitosan/PGA hollow spheres of various sizes along with a range of surface charges, and to evaluate effect of both size and surface charge on the cellular viability, blood compatibility and cellular internalization behavior of these hollow spheres. The influence of size was determined by fabricating four different sizes of spheres: 100, 300, 500 and 1000nm (Figure 1), while the effect of surface charge was investigated by creating negative, neutral and PEGylated surface modified spheres. Human umbilical vein endothelial cells (HUVECs) and human umbilical artery smooth muscle cells (HUASMCs) were chosen for this experiment as model cell types.

2. Materials and Methods

2.1. Materials

All reagents were purchased from Sigma-Aldrich (Dublin, Ireland) unless otherwise noted. PS beads 100 and 300 nm, sulphuric acid, chitosan (low molecular weight, 90% of deacetylation), ethanol, acetic acid, tetrahydrofuran (THF), PGA, phosphate buffered saline (PBS), 2-(*N*-morpholino)ethanesulfonic acid (MES), *N*-hydroxysuccinimide (NHS) and trypsin-EDTA,

methylthiazolyldiphenyl-tetrazolium bromide (MTT), 1-ethyl-3-(3-dimethylaminopropyl) carbodiimide (EDC) and 2,methoxy ethylamine (MEA). PS beads 510 and 1000nm from GENTAUR (Brussels, Europe). PA series polyethylene glycol (PEG) (3400 Da) from Sunbright (NOF corporation, Japan), agar low viscosity resin kit Agar Scientific Ltd. (Essex, UK). K3E and 9NC vacutainers from BD (Dublin, Ireland), enzyme linked immunosorbent assay (ELISA) kit for human soluble P-selectin (sP-selectin) immunoassay from R&D Systems (Minneapolis, USA). Human C3a ELISA kit BD OptEIA™ from BD Biosciences-Pharmanigen (San Jose, CA, USA), fluorescein isothiocyanate (FITC), TO-PRO-3 iodide and bovine serum albumin (BSA) from Invitrogen (Dublin, Ireland). Endothelial cell growth medium-2 (EGM-2) and smooth muscle cell growth media (SmGM-2) along with growth factors and cytokines from Lonza (England, UK).

2.2. Fabrication of Different Sizes of Hollow Spheres and FITC Labelling

Chitosan/PGA hollow spheres were fabricated as described in the protocol [4]. Briefly, a 0.5wt% solution of chitosan in 1% (v/v) acetic acid was added to a colloidal solution of sulfonated PS beads of various sizes (100, 300, 500 and 1000nm) and the mixture was then shaken for 24 h at 4 ºC. PGA (1.7 equivalent) in MES (0.05M, pH 5.5) was mixed for five minutes with NHS (0.8eq.) and EDC (0.8eq.). This was then added to the chitosan/polystyrene solution and the solution was stirred for 24 h. Cross-linking reaction occurred over a 24 h. To obtain a surface negative charge on the native hollow spheres an additional 0.7 equivalent PGA was added to chitosan during the fabrication process. Finally, to obtain hollow spheres, PS cores were dissolved with THF and dried under vacuum to evaporate excessive solvent. Spheres were observed under transmission electron microscopy for analyzing their internal structure and size. FITC labelling was performed as described in our previous study [4]. PGA was labelled with FITC prior to cross-linking step during the hollow sphere fabrication process. Briefly, a weight ratio of 1:40 of FITC to PGA was kept shaking at 4 ºC for overnight. The unbound FITC molecules were removed by dialyzing. FITC labelled PGA was then used to fabricate the hollow spheres.

2.3. Alteration of Surface Charge and Function of Hollow Spheres

Spheres of all the four sizes were used for surface modifications. For neutralization, native spheres were covalently cross-linked with MEA. Briefly, 50mg of chitosan/PGA hollow spheres (0.086 mmol of carboxylic group) were dispersed in MES buffer (2-3ml, pH 5.5) in a round bottom flask and 22.24µl of MEA (0.258 mmol of amino group), EDC (0.172 mmol) and NHS (0.172 mmol) were then added. The mixture was stirred overnight at room temperature and dialyzed to remove the unreacted chemicals. Surface PEGylation of these hollow spheres was performed using propylamine-functionalized amino-terminated PEG. 0.043 mmol of PEG was mixed with 0.086 mmol hollow spheres with EDC (0.086 mmol) and NHS (0.086 mmol) in MES buffer (pH 5.5). The mixture was then stirred overnight and dialyzed to remove unreacted chemicals. Surface charge was analyzed in mV using zeta sizer (NanoZS, Malvern) after surface modifications of all the spheres.

2.4. Cell Maintenance

HUVECs and HUASMCs were grown in T75 flasks using EGM-2 and SmGM-2 media respectively and incubated at 37 °C in an atmosphere of 5% CO_2. The culture medium was changed every 36 h. The cells were harvested and sub-cultured when > 80% confluency was observed.

2.5. Cell Viability Study

Cells were seeded in 96 well plates. Spheres (all 12 parameters) were added to each cell type (HUVEC and HUASMC) and incubated for different time point at 6, 12, 24 and 48 h. 50µl MTT was added to each sample 3 h prior to completion of time course (e.g. for 12 hour time point, MTT added at 9 h for 3 h incubation). Finally, 100µl DMSO was added, and read at 570nm. Results were expressed as a percentage of cell viability of treated samples compared to non-treated cells (100%) over specified time course.

2.6. Cellular Internalization Behaviour of Spheres

2.6.1. Characterization by Confocal Imaging

In order to visualize the spheres within HUVECs and HUASMCs, confocal microscopy was performed. Cells were incubated with FITC labelled hollow spheres for desired time point and then fixed with paraformaldehyde (4%) and stained for cytoskeleton using rhodamine phalloidin.

2.6.2. Characterization by Transmission Electron Microscopy

Internalization and co-localization of spheres was characterized by transmission electron microscopy (TEM). Cells were incubated with 50 µg of spheres for 24 h. After incubation, cells were washed and fixed with paraformaldehyde, dehydrated by using a gradient of ethanol and then embedded into resin. After polymerisation of the resin (3 days at 60 °C), cut section of 90nm thickness were done using an ultramicrotome and samples were then analyzed using TEM.

2.6.3. Quantification by Flow Cytometry

Cells were grown in T25 tissue culture flasks for flow cytometry studies and spheres at a concentration of 50µg/ml concentration were added. After the desired incubation time, cells were trypsinized and resuspended in a buffer (1% BSA in PBS). Cells were then analyzed using flow cytometry for internalization efficiency.

2.6.4. Quantification by High Content Analysis

HUVECs and HUASMCs were seeded on 96 well plates for high content analysis (HCA). FITC-hollow spheres were seeded and incubated for different time points 6, 12, 24 and 48 h. After the desired incubation times cells were fixed and stained for nucleus using TO-PRO-3 iodide. Finally, the plates were read using *In Cell Analyzer 1000* GE Healthcare for 420nm (FITC) and 620nm (TO-PRO-3 iodide).

2.7. Blood Compatibility

Human blood was drawn from healthy volunteers into vacutainers containing either EDTA or sodium citrate and tested with all four different sizes and surface modified modifications to elucidate the effect of size and surface charge of hollow spheres on various components of blood and to determine their effect on erythrocytes, coagulation and the complement system. Ethical

approval for this study was granted by the Human Ethics Committee of the National University of Ireland, Galway.

2.7.1. Haemolysis

EDTA-anticoagulated blood was centrifuged for 5 min at a speed of 900g. The serum fraction was removed and the volume was raised to its original using 150mM NaCl. This step was repeated twice and the final suspension was diluted 1:10 with 100mM phosphate buffer. 2 x 10^8 red blood cells/ml were incubated with various sizes and charge of spheres each at a final concentration of 40µg/ml. PBS was used as a negative control whereas Triton X-100 1% (w/v) was used as a positive control. All samples were incubated under gentle agitation for 2 hours at 37 $^{\circ}$C and centrifuged at 900g for 5 min. The absorbance of the supernatant was measured for release of haemoglobin at 545nm.

% Haemolysis was calculated as follows:

$$\% \text{ Haemolysis} = \frac{\text{Absorbance of test sample} - \text{Absorbance of control}}{\text{Highest absorbance for positive control}} \text{ X } 100$$

2.7.2. Platelet Activation

Whole blood was centrifuged at 85g for 15 min to remove platelet-rich supernatant. The remaining blood was again centrifuged for 10 minutes at 140g and mixed with the previous extracted plasma to get platelet rich plasma (PRP). Platelet poor plasma PPP was obtained by centrifuging the remaining blood for 5 min at 800g. The PRP was then diluted 1:100 with 1 % ammonium oxalate and adjusted to a final platelet concentration of 6 x 10^8/ml. 300µl of PRP was incubated with 40µg of hollow spheres from all different sizes and surface modifications for 1 h at 37 $^{\circ}$C. The supernatant was then centrifuged at 2000g for 10 min. Platelet activation was measured by the concentration of sP-selectin levels in the plasma and was determined using ELISA kit according to the manufacturer's protocol. Both PPP and PRP were used as control.

2.7.3. Complement System

To assess complement activation, the cleavage of complement component C3 was monitored by measuring the formation of its activation peptide; C3a desArg, using a commercial C3a enzyme immunoassay kit (BD Bioscience). Activation studies were performed using pooled citrated plasma isolated by centrifugation from whole blood donations. Equal volumes of plasma and spheres in saline were incubated at 37 °C for 1h. Briefly, the samples were diluted with the dilution buffer provided in the kit and added to a microtiter plate coated with a monoclonal antibody specific for human C3a desArg. After one hour incubation at room temperature to allow any C3a in the sample to bind to the monoclonal antibody, the plates were washed and incubated with peroxidase-conjugated rabbit anti-C3a for 15 min. Following a final wash step, the chromogenic substrate was added to detect the bound C3a. Absorbance was measured at 450nm. The sample C3a concentrations were calculated using a standard curve with net absorbance values plotted on the y-axis for each C3a concentration indicated on the x-axis. Sample values were accepted as valid if they fell on the standard curve; sample values above the top end of the curve were retested following further dilution. Measurements were performed in duplicate.

2.7.4. Plasma Clotting Time

Howell's method was employed to investigate plasma recalcification time (PRT). Blood was collected in a sodium-citrate vacutainers. It was then centrifuged at 3000 rpm at 8 $^{\circ}$C for 20 min to obtain the platelet-poor plasma (PPP). 0.1ml of the PPP and 40 µg of samples suspended in PBS were incubated at 37 $^{\circ}$C for 5 min in a 96 well plate. 0.1ml of 0.025 M $CaCl_2$ solution was then added and the plasma solution was monitored for clotting by manually dipping a stainless-steel wire hook coated with silicone into the solution, to detect fibrin threads. Clotting times were recorded as the time at which first fibrin strand formed on the hook.

3. Results

3.1. Size and Surface Charge Analysis

Size analysis of hollow spheres was carried using TEM. Monodisperse hollow spheres were obtained for all the sizes (Figure 2). The size of hollow spheres was 110 ± 7.8nm, 315 ± 10.4nm, 508 ± 7.6nm, and 990 ± 70nm for 100, 300, 500 and 1000nm polystyrene beads used respectively. Zeta potential analysis was used to characterize the surface modification. Native spheres characterized previously [4] (prepared with an excess of 0.7 eq. of PGA) had a resultant negative potential of between -35 and -40 mV for all sizes. Neutralization of the negatively charged spheres using MEA was achieved, with an approximately neutral value of zeta potential of - 4 mV. Polyethylene glycol (PEG) engraftment on the surfaces was also verified; as the quantity of PEG was less than MEA, an adjustment of the zeta potential to -20 mV was observed, indicating that half of the carboxyl groups on the surface of the native spheres were used to link the PEG moiety (Figure 3). There was no significant difference in size was found after surface modifications of spheres (Data not shown).

3.2. Cell Viability

Results related to cell viability are provided as supplementary information. The data suggests good cell viability for all the spheres and have been discussed briefly about their size, surface charge and cell type effect later in the discussion section.

3.3. Cellular Internalization Behaviour

3.3.1. Co-localization

Confocal micrographs show co-localization of the negatively charged FITC labelled spheres (green) within HUVECs and HUASMCs after 24 h incubation (Figure 4). Confocal micrographs of 1000nm spheres are not shown in this report as there was negligible internalization of this size of sphere. 100nm and 300nm spheres can be seen in the perinuclear region of the cells. Flow cytometry and fluorescence microscope only detect gross fluorescence that emits from cells; highly dispersed hollow spheres, such as single sphere, might not be detectable by either technique. The cell uptake of single hollow spheres must be investigated by other methods, such as TEM. Cells incubated with

100nm neutral hollow spheres for 24 h were observed under TEM (Figure 5). TEM micrographs show hollow spheres inside lysosome of both the cell types (Figure 5A and B). Figure 5C illustrates the endocytic pathway of hollow spheres from early endosome to lysosome inside HUVEC.

3.3.2. Flow Cytometric Analysis of Cellular Internalization

The impact of size and surface charge on cellular internalization was quantified at 12 h following incubation using flow cytometry. Figure 6 shows internalization efficiency of spheres within HUVECs (Figure 6A) and HUASMCs (Figure 6B). 100nm neutral spheres showed increased internalization in both cell types with 76 % in HUVECs and 56 % in HUASMCs. HUASMCs had reduced sphere uptake than HUVECs in all the sizes and surface modifications investigated. 300 and 500nm spheres show similar internalization efficiency in both HUVECs and HUASMCs. 1000nm spheres, regardless of surface charge had low internalization with 9-13% internalization in both cell types investigated. For all the sizes, negatively charged spheres presented the lowest uptake profile.

3.3.3. High Content Analysis of Cellular Internalization

HCA enabled quantitative estimation of the internalization of FITC labelled nanospheres of different parameters, including size, surface charges and time points within HUVECs and HUASMCs. Cellular internalization was estimated in terms of relative fluorescence. The results found that 100nm neutral spheres were significantly more internalized ($p < 0.05$) when compared with other sizes, for PEGylated and neutrally charged spheres in both cell types, which is consistent with flow cytometric data, and showed a constant increase of internalization over time from a relative fluorescence value of 6 to 18 in HUVECs (Figure 7). Internalization is reduced in HUASMCs for all sizes and surface charges (Figure 8). PEGylated 100nm nanospheres show the same level of internalization with HUVECs and HUASMCs with an approximate relative fluorescence value of 8. Negatively charged spheres for all sizes resulted in less internalization in both type of cells. Also, neutral, PEGylated and negatively charged spheres of 1000nm size had

much less uptake for all the time points. Overall, the interaction of 100nm nanospheres with both cell types result in a higher degree of internalization compared to the 300, 500 and 1000nm size nanospheres. The effect of size on internalization is inversely related [29, 30] while the neutrally charged sphere seems to be more relevant than PEGylated and negatively charged spheres for internalization. HUASMCs seem more resistant to internalization of hollow spheres rather than HUVECs.

3.4. Blood Compatibility

A major challenge for the systemic delivery of synthetic vehicles for gene delivery is their lack of stability in the blood stream, their degradation, and clearance by the reticuloendothelial system, which makes the elucidation of their interaction with blood components essential. Several interactions with the family of spheres were investigated to determine the potential systemic delivery *in vivo* of the hollow spheres.

3.4.1. Haemolysis

In vitro analysis of red blood cells lysis is an established method to determine effect of materials with erythrocytes. During this analysis, phosphate buffered saline (PBS) was used as a negative control (0 %) and TritonX (detergent) as a positive control (100 %) of haemolysis. Negatively charged spheres have a significantly higher % haemolysis at sizes 300, 500 and 1000nm whereas PEGylated spheres have a significantly reduced % haemolysis at these sizes. 100nm spheres have a significantly reduced % haemolysis for all surface charges (Figure 9). Irrespective of size or surface charge, all spheres have a negligible effect on haemolysis (1 %).

3.4.2. Platelet Activation

Platelet activation upon interaction with particles is another indication of blood incompatibility as it could lead to thrombotic complications under *in vivo* conditions. It is known that polycations induce aggregation and activation of platelets, and this can impair platelet function [31]. In this study, platelet activation was quantified by the release of soluble P-selectin (sP-Selectin) after incubation

with all spheres. PBS was used as a negative control. The results found that size does not have a significant influence on the platelet activation. Negatively charged spheres however, induce a significantly higher level of sP- selectin ($p < 0.05$) when compared to other neutral and PEGylated spheres for all sizes (Figure 10).

3.4.3. Complement System Activation

Complement activation is an extremely important factor when considering synthetic cationic vehicles for delivery. Activation of components of the complement system could produce anaphylatoxins which lead to activation of the immune system [32]. Opsonization of synthetic carriers with complement components such as C3a and C5a could eventually lead to the clearance of such particles by the reticuloendothelial system which makes the elucidation of this interaction significant. In this study complement activation was investigated by quantifying the release of C3a after incubation with spheres. PBS was used as a negative control and no significant difference was observed between samples and the control (Figure 11).

3.4.4. Plasma Clotting Time

The clotting process utilizes the intrinsic and extrinsic pathway which ultimately leads to clot formation. The intrinsic pathway is initiated when blood comes into contact with a surface, while the extrinsic pathway is initiated upon vascular injury which leads to exposure of tissue factor (TF). Plasma recalcification profiles are used to mimic the intrinsic coagulation system *in vitro*. PBS was used as a negative control in this study. To quantify plasma recalcification profiles, $T_{1/2\ max}$ was calculated as the time at which half the saturate absorbance was reached. Clotting times are significantly shorter ($p < 0.05$) for all samples when compared to the control (12.3 ± 0.3 mins). Negatively charged spheres significantly decreased clotting times compared to other surface charges at 100 and 300nm spheres. The absence of a significant effect at larger sphere size indicates that there is a size at which surface charge does not have an effect. The effect of size did not have a significant effect on the clotting time of PEGylated spheres whereas 300nm spheres had a reduced

clotting time when surface charge was negative and neutral when compared to 500 and 1000nm spheres (Figure 12).

4. Discussion

A wide family of hollow spheres, with the potential to deliver drugs, compounds and/or genetic material has been developed so far in terms of size and surface charge. Sizes ranging between 100 and 1000nm were prepared and samples were modified to obtain neutral surface charge and PEGylated surfaces or less negative surface charge. In order to evaluate the potential of these hollow spheres to be used as a delivery vehicle, cytotoxicity, cellular internalization and blood compatibility were investigated (Table 1). Surface charge and size exerted a significant influence on the sphere's behaviour, most notably on haemolysis, platelet activation, plasma recalcification time, toxicity and cellular uptake over time. Smaller sizes (100nm spheres) have a better compatibility profile with lower haemolysis and platelet activation. Surface charge has a stronger influence on plasma recalcification time than size, whereas PEGylated spheres do not significantly reduce clotting times. HUVECs and HUASMCs have different cytotoxicity responses when incubated with the spheres which were quantified using MTT assay (Supplementary Figures 1-4). Size and surface charge had no significant effect on HUASMCs when compared with controls (Supplementary Figure 2 and 4). However, surface charge had a significant effect on the viability of HUVECs (Supplementary Figure 1 and 3). The effect of surface charge was not significant with 1000nm spheres; however for 100, 300 and 500nm spheres surface charge had a significant effect ($p < 0.01$). Negatively charged 100nm spheres had greater viability compared to neutral and PEGylated spheres. However there was a transition to neutral and then PEGylated spheres having greater viability with HUVECs at sizes 300 and 500nm respectively. This suggests that there is a synergistic relationship between the size and surface charge that dictates their cytotoxicity. 1000nm spheres had the highest viability with PEGylated and neutral charge spheres ($p < 0.05$). However, there was no significant difference between 100 and 1000nm spheres when the surface charge was

negative. This is attributed to the low internalization of 100nm negatively charged spheres within the cells. Cellular uptake is significantly dependant on size and surface charge and 100nm appears to be an optimum size for internalization for neutral and PEGylated spheres. Cellular internalization is also dependent on parameters, e.g. size, surface charge, incubation time and also the cell type. HUVECs and HUASMCs show different internalization behaviours with these spheres over different time points, varying size and charge. This is supported by flow cytometry and HCA data. 100nm and other spheres show relatively increased uptake within HUVECs compared to that of HUASMCs, with the exception of 1000nm spheres, where internalization is insignificant for both cell types. 100nm neutral spheres have more uptake than 100nm PEGylated spheres; whereas there is no significant difference of internalization between 300nm and 500nm neutral and PEGylated spheres. This indicates that there is a size limit after which surface modification has no influence on cellular internalization. Positive charge of the cell membrane is an obvious reason for the low internalization of negatively charged spheres and hence internalization of spheres into cells requires a holistic approach that takes into account of size and surface charge.

5. Conclusions

FITC labelled chitosan/PGA hollow spheres with definite sphere size, surface charge, were created for elucidating the combinatorial effects of physicochemical properties on cellular internalization, cell viability and blood compatibility. This is the first study in literature that reports the combinatorial effect of the parameters. It was clear that physicochemical differences such as alternation of size and zeta potential played a vital role in internalisation behaviour of hollow spheres as well as on cell viability and blood compatibility. FITC labelled negative, neutral and PEGylated hollow spheres showed cell-line-dependent internalization behaviour. The results were in agreement with those of inorganic spheres and liposomes, indicating that size and surface charge of spheres are more important parameters than sphere's composition. Therefore, results obtained using tunable chitosan/PGA hollow spheres as a model system in the present investigation could be

applied for other types of solid spheres as well as hollow spheres. These results are of potential value to serve as guidelines for predicting the behaviour of spheres for specific desired applications in biological and pharmaceutical fields, including design of nano to submicron sized delivery vehicles.

Acknowledgements

This work was supported by Science Foundation Ireland under Grant No. 07/SRC/B1163 and Debra Ireland (Dystrophic Epidermolysis Bullosa Research Association).The authors would also like to acknowledge Paul Fullard for his contribution in graphics and Pierce Lalor for assistance in microscopy techniques.

Appendix:

Supplementary Data

Supplementary data associated with this article can be found in the online version.

References

[1] Meier W. Polymer nanocapsule. Chem Soc Rev 2000; 29: 295-303.

[2] Lensen D, Vriezema DM, van Hest JC. Polymeric microcapsules for synthetic applications. Macromol Biosci 2008; 8(11): 991-1005.

[3] Zelikin AN, Becker AL, Johnston AP, Wark KL, Turatti F, Caruso F. A general approach for DNA encapsulation in degradable polymer microcapsules. ACS Nano 2007; 1(1): 63-9.

[4] Rethore G, Mathew A, Naik H, Pandit A. Preparation of chitosan/polyglutamic acid spheres based on the use of polystyrene template as a nonviral gene carrier. Tissue Eng Part C Methods 2009; 15(4): 605-13.

[5] Kuykendall DW, Zimmerman SC. Nanoparticles: a very versatile nanocapsule. Nat Nanotechnol 2007**;** 2(4): 201-2.

[6] Kim E, Kim D, Jung H, Lee J, Paul S, Selvapalam N, et al. Facile, template-free synthesis of stimuli-responsive polymer nanocapsules for targeted drug delivery. Angew Chem Int Ed Engl 2010; 49(26): 4405-8.

[7] Rethore G, Pandit A. Use of templates to fabricate nanoscale spherical structures for defined architectural control. Small 2010; 6(4): 488-98.

[8] Caruso F, Caruso RA, Mohwald H. Nanoengineering of inorganic and hybrid hollow spheres by colloidal templating. Science 1998; 282(5391): 1111-4.

[9] Alexis F, Pridgen E, Molnar LK, Farokhzad OC. Factors affecting the clearance and biodistribution of polymeric nanoparticles. Mol Pharm 2008; 5 (4): 505-15.

[10] Chono S, Tanino T, Seki T, Morimoto K. Uptake characteristics of liposomes by rat alveolar macrophages: influence of particle size and surface mannose modification. J Pharm Pharmacol 2007; 59(1): 75-80.

[11] Osaki F, Kanamori T, Sando S, Sera T, Aoyama Y. A quantum dot conjugated sugar ball and its cellular uptake: on the size effects of endocytosis in the subviral region. J Am Chem Soc 2004; 126(21): 6520-1.

[12] Win KY, Feng SS. Effects of particle size and surface coating on cellular uptake of polymeric nanoparticles for oral delivery of anticancer drugs. Biomaterials 2005; 26(15): 2713-22.

[13] Foged C, Brodin B, Frokjaer S, Sundblad A. Particle size and surface charge affect particle uptake by human dendritic cells in an in vitro model. Int J Pharm 2005; 298 (2): 315-22.

[14] Chithrani BD, Ghazani AA, Chan WC. Determining the size and shape dependence of gold nanoparticle uptake into mammalian cells. Nano Lett 2006; 6(4): 662-8.

[15] Jiang W, Kim BY, Rutka JT, Chan, WC. Nanoparticle-mediated cellular response is size-dependent. Nat Nanotechnol 2008; 3(3): 145-50.

[16] Lu F, Wu SH, Hung Y, Mou CY. Size effect on cell uptake in well-suspended, uniform mesoporous silica nanoparticles. Small 2009; 5(12): 1408-13.

[17] Lee KD, Nir S, Papahadjopoulos D. Quantitative analysis of liposome-cell interactions in vitro: rate constants of binding and endocytosis with suspension and adherent J774 cells and human monocytes. Biochemistry 1993; 32(3): 889-99.

[18] Warheit DB. How meaningful are the results of nanotoxicity studies in the absence of adequate material characterization? Toxicol Sci 2008; 101(2): 183-5.

[19] Murdock RC, Braydich-Stolle L, Schrand AM, Schlager JJ, Hussain SM. Characterization of nanomaterial dispersion in solution prior to in vitro exposure using dynamic light scattering technique. Toxicol Sci 2008; 101(2): 239-53.

[20] Prabhu BM, Ali SF, Murdock, RC, Hussain SM, Srivatsan M. Copper nanoparticles exert size and concentration dependent toxicity on somatosensory neurons of rat. Nanotoxicology 2010; 4(2): 150-60.

[21] Napierska D, Thomassen LC, Rabolli V, Lison D, Gonzalez L, Kirsch-Volders M, et al., Size-dependent cytotoxicity of monodisperse silica nanoparticles in human endothelial cells. Small 2009; 5(7): 846-53.

[22] Wittmaack K. In search of the most relevant parameter for quantifying lung inflammatory response to nanoparticle exposure: particle number, surface area, or what? Environ Health Perspect 2007; 115(2): 187-94.

[23] Gojova A, Guo B, Kota RS, Rutledge JC, Kennedy IM, Barakat AI. Induction of inflammation in vascular endothelial cells by metal oxide nanoparticles: effect of particle composition. Environ Health Perspect 2007; 115(3): 403-9.

[24] Mayer A, Vadon M, Rinner B, Novak A, Wintersteiger R, Frohlich E. The role of nanoparticle size in hemocompatibility. Toxicology 2009; 258(2-3): 139-47.

[25] Gratton SE, Ropp PA, Pohlhaus PD, Luft JC, Madden VJ, Napier ME, et al. The effect of particle design on cellular internalization pathways. Proc Natl Acad Sci USA 2008; 105(33): 11613-8.

[26] Cortez C, Tomaskovic-Crook E, Johnston AP, Scott AM, Nice EC, Heath JK, et al. Influence of size, surface, cell line, and kinetic properties on the specific binding of A33 antigen-targeted multilayered particles and capsules to colorectal cancer cells. ACS Nano 2007; 1(2): 93-102.

[27] Zauner W, Farrow NA, Haines AM. In vitro uptake of polystyrene microspheres: effect of particle size, cell line and cell density. J Control Release 2001; 71(1): 39-51.

[28] Clift MJ, Rothen-Rutishauser B, Brown DM, Duffin R, Donaldson K, Proudfoot L, et al., The impact of different nanoparticle surface chemistry and size on uptake and toxicity in a murine macrophage cell line. Toxicol Appl Pharmacol 2008; 232(3): 418-27.

[29] Chung T-H, Wu S-H, Yao M, Lu C-W, Lin Y-S, Hung Y, et al., The Effect of Surface Charge on the Uptake and Biological Function of Mesoporous Silica Nanoparticles in 3T3-L1 Cells and Human Mesenchymal Stem Cells. Biomaterials 2007; 28(19): 2959-66.

[30] Rejman J, Oberle V, Zuhorn IS, Hoekstra D. Size-dependent internalization of particles via the pathways of clathrin and caveolae-mediated endocytosis. Biochem. J 2004; 377: 159-69.

[31] Sushkevich GN, Dubovik BV, Baluda VP, Étlis VS, Shomina FN. Synthetic polycations as activators of the endogenous mechanism of platelet aggregation. Bull Exp Biol Med 1977; 83(5): 627-30.

[32] Dawson P, Turner MW, Bradshaw A, Westaby S. Complement activation and generation of C3a anaphylatoxin by radiological contrast agents. Br J Radiol 1983; 56(667): 447-8.

Figure Captions

Figure 1: Schematic representation of hollow sphere fabrication and surface modifications

Figure 2: Chitosan/PGA hollow spheres observed under TEM. (A) 100nm (B) 300nm (C) 500nm (D) 1000nm hollow spheres

Figure 3: Zeta potential analysis of spheres showing net chanrge after surface modifications of all spheres. Data is represented as the mean ± standard deviation (n = 3). * indicates a statistically significant different between samples with $p < 0.05$

Figure 4: Confocal micrographs of FITC labelled spheres (A) 100nm and (B) 300nm internalized into HUVECs and (C) 100nm and (D) 300nm internalized into HUASMCs. All images were taken after 24 h incubation with cells

Figure 5: TEM images illustrating 100nm neutrally charged spheres internalized into (A) HUVECs and inset shows the hollow spheres inside lysosome and (B) HUASMCs and inset shows hollow spheres inside lysosome. (C) Higher Magnification image of (A) showing endocytic internalization of hollow spheres from endosome (E) to lysosmes (L) near nucleus (N).

Figure 6: Flow cytometry data, elucidating the effect of size and surface modifications on the internalization efficiency of spheres into (A) HUVECs and (B) HUASMCs at 12 h incubation

Figure 7: High content analysis showing internalization of PEGylated, neutral and negatively charged spheres with HUVECs over a time course period of 6, 12, 24 and 48 h. Data is represented as the mean ± standard deviation (n = 3, $p < 0.05$)

Figure 8: High content analysis showing internalization of PEGylated, neutral and negatively charged spheres with HUASMCs over a time course period of 6, 12, 24 and 48 h. Data is represented as the mean ± standard deviation (n = 3, $p < 0.05$)

Figure 9: % Haemolysis after incubation with human erythrocytes with (A) effect of size and (B) effect of surface charge. Data is represented as the mean ± standard deviation (n = 4). * indicates a statistically significant different between samples with $p < 0.05$

Figure 10: Platelet activation as indicated by sP-Selectin release (A) effect of size and (B) effect of surface charge. Data is represented as the mean ± standard deviation (n = 4). * indicates a statistically significant different between samples with $p < 0.05$

Figure 11: Complement activation as indicated by C3a release (A) effect of size and (B) effect of surface charge. Data is represented as the mean ± standard deviation (n = 4). * indicates a statistically significant different between samples with $p < 0.05$

Figure 12: Plasma recalcification time, quantified using calculation of the point at which the recalcification profile reaches half of the maximum absorbance value with (A) showing effect of size (B) showing effect of surface charge. Data is

represented as the mean ± standard deviation (n = 4). * indicates a statistically significant difference ($p < 0.05$), ** indicates a statistically significant difference ($p < 0.01$)

Table

	Negative				Neutral				PEGylated			
	100	300	500	1000	100	300	500	1000	100	300	500	1000
Haemolysis	-	+++	+++	+++	-	++	+	++	-	++	++	+
Platelet Activation	+++	+++	-	+++	-	-	-	-	-	-	-	-
Complement Activation	-	-	-	-	-	-	-	-	-	+	-	-
Plasma Recalcification Time	++	+++	-	-	-	+	-	-	-	-	-	-
Cytotoxicity												
HUVEC	-	++	+	-	-	+	++	-	+	+	+	-
HUASMC	-	-	-	-	-	-	-	-	-	-	-	-
Internalization												
HUVEC	-	-	-	-	+++	++	+	-	+++	++	+	-
HUASMC	-	-	-	-	++	+	-	-	++	+	-	-

Table 1: Summary of effect of size and surface charge on all parameters investigated

Figure 1

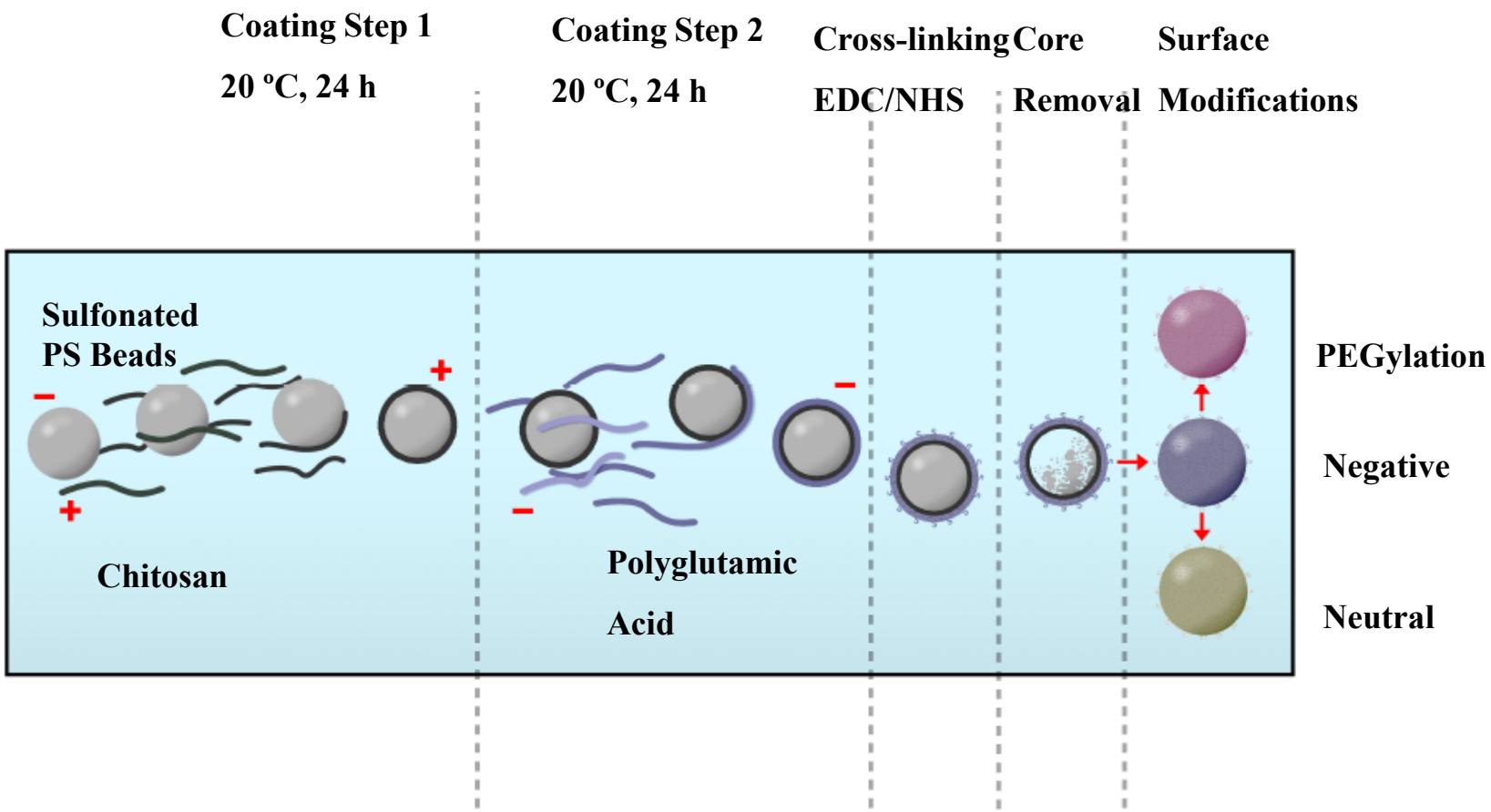
Coating Step 1
20 °C, 24 h
Coating Step 2
20 °C, 24 h
Cross-linking
EDC/NHS
Core
Removal
Surface
Modifications
Sulfonated
PS Beads
Chitosan
Polyglutamic
Acid
PEGylation
Negative
Neutral

Figure

Click here to download high resolution image

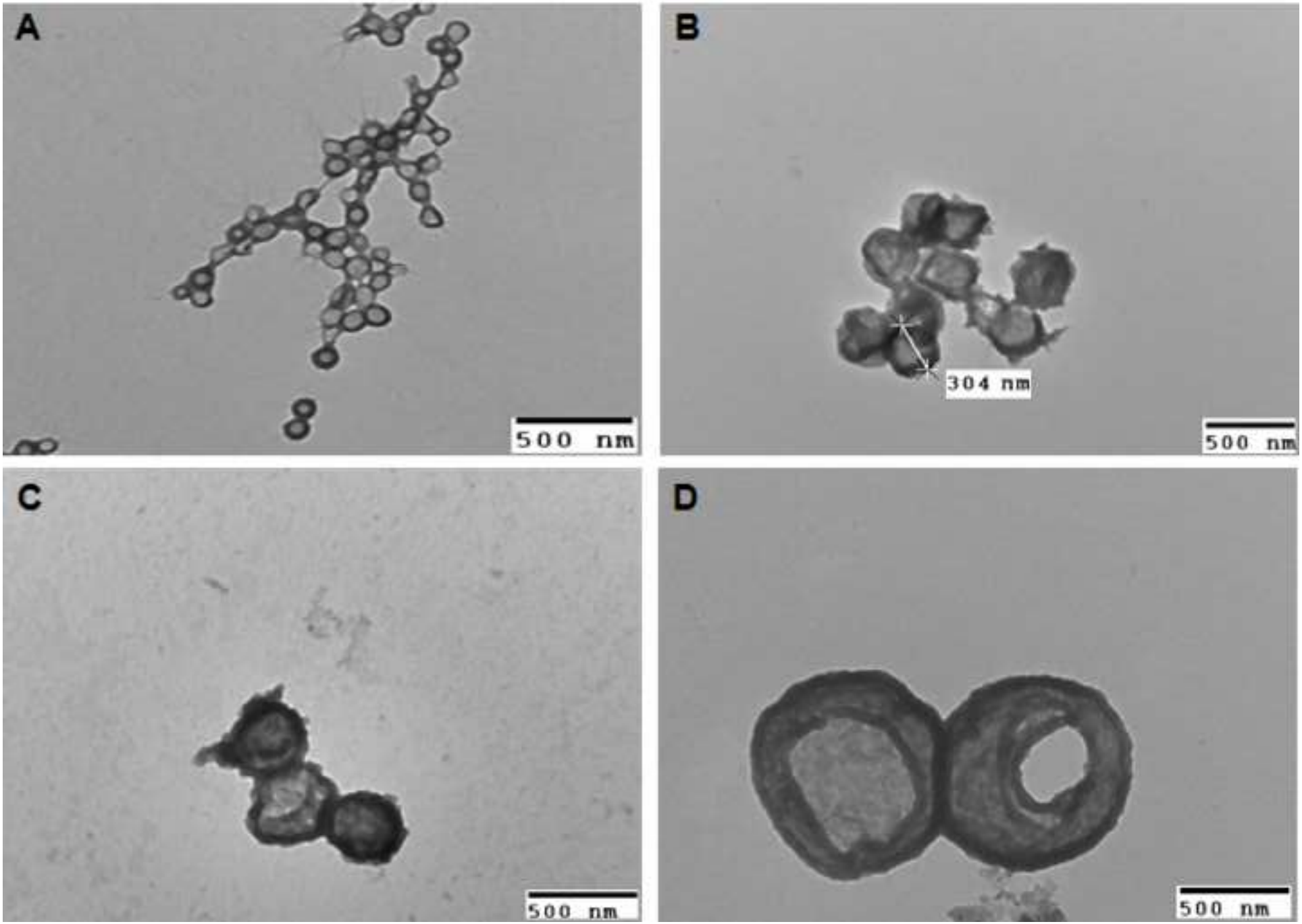

Figure 3

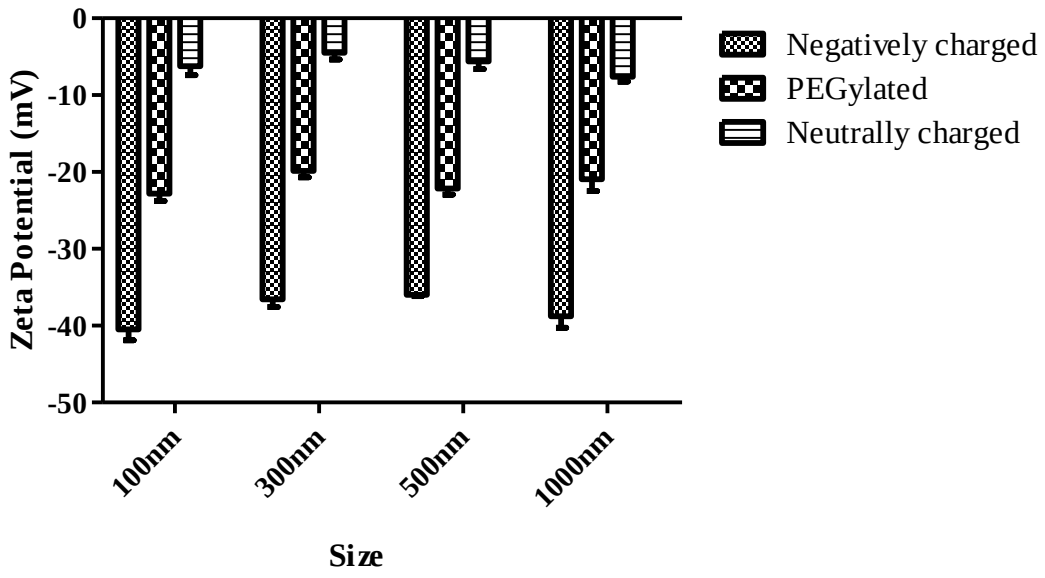
0
-10
-20
-30
-40
-50
Zeta Potential (mV)
100nm
300nm
500nm
1000nm
Size
Negatively charged
PEGylated
Neutrally charged

Figure

Click here to download high resolution image

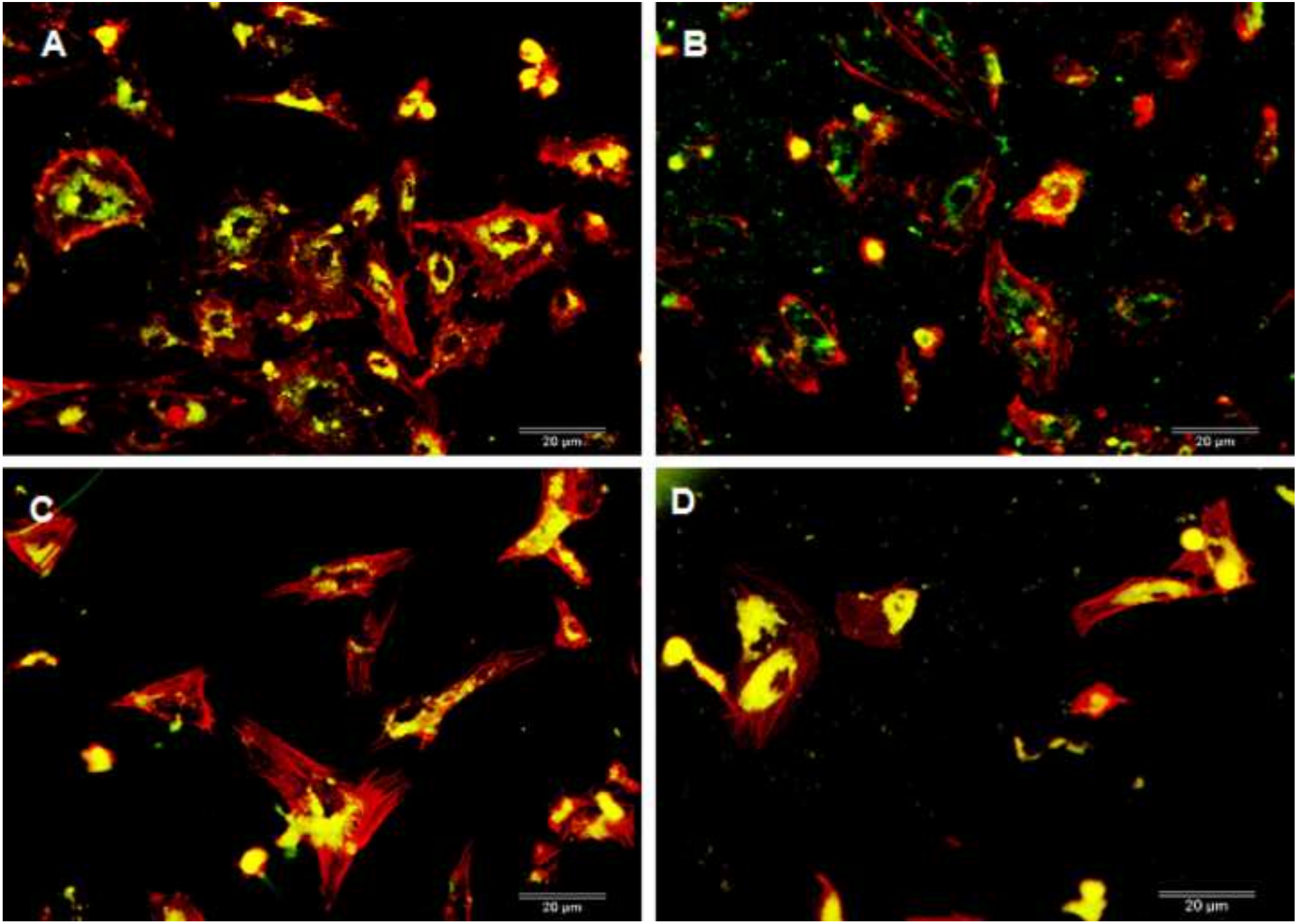

Figure

Click here to download high resolution image

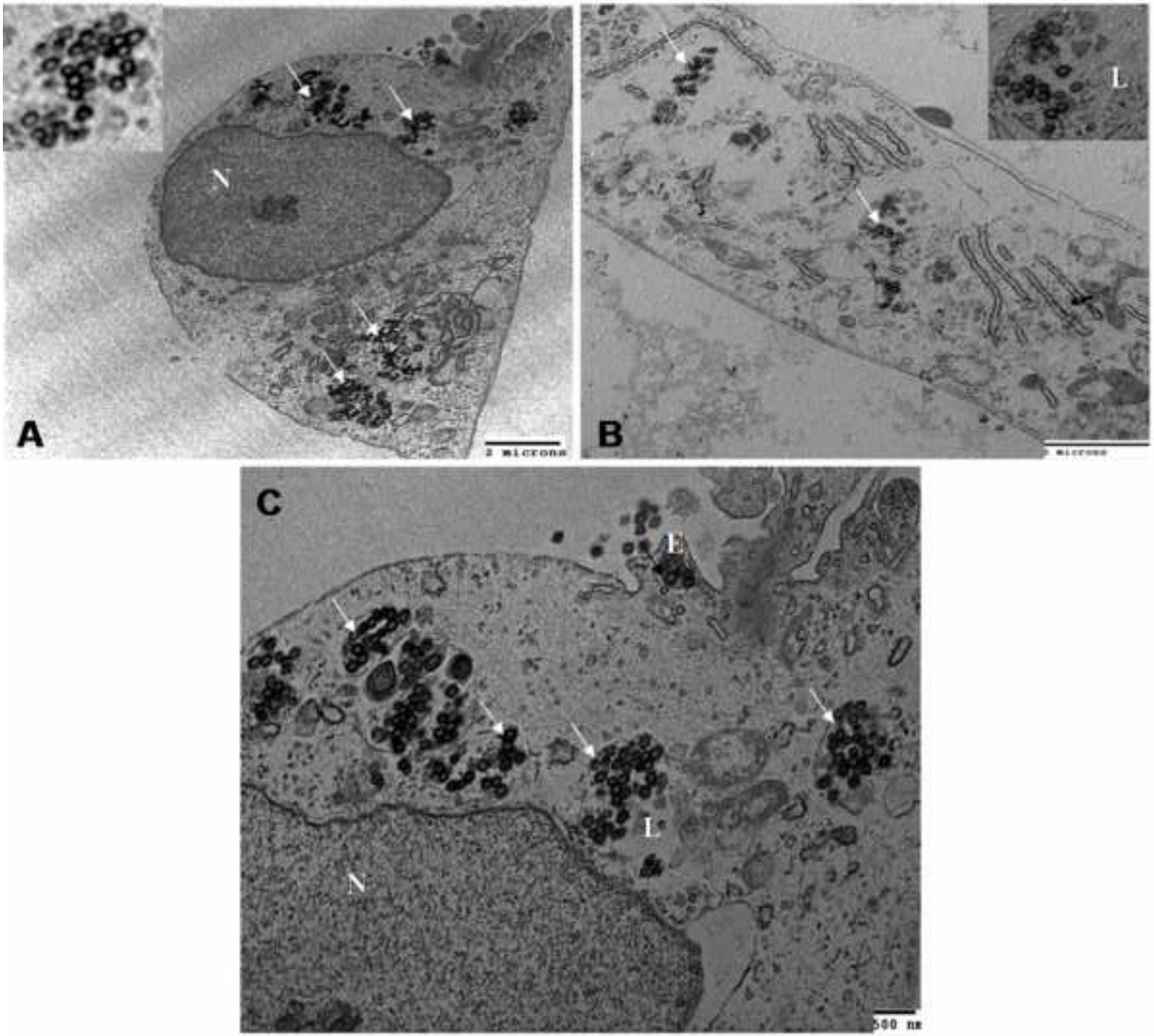

Figure 6

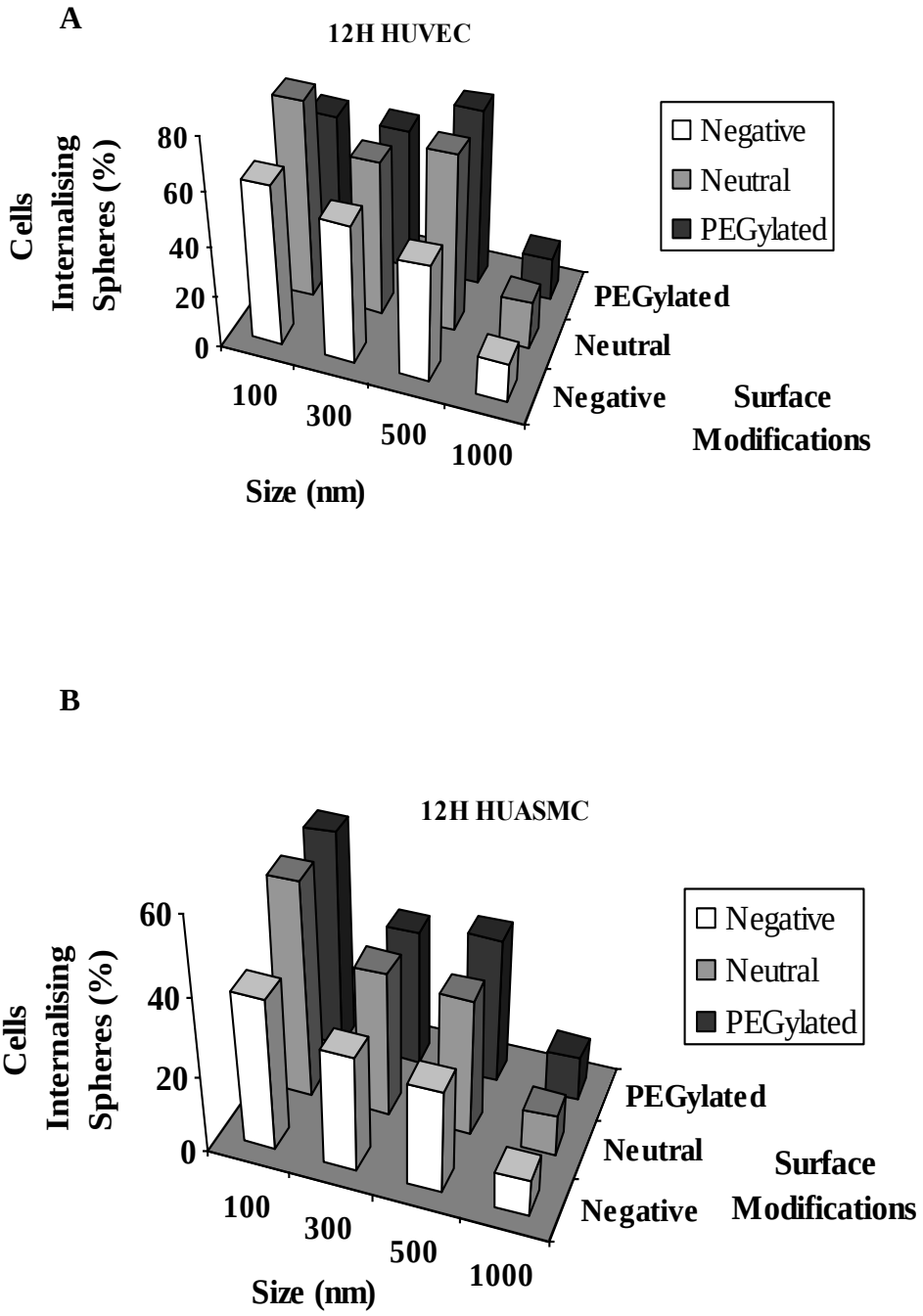
A
12H HUVEC
Cells Internalising Spheres (%)
80
60
40
20
0
100
300
500
1000
Size (nm)
Negative
Neutral
PEGylated
PEGylated
Neutral
Negative
Surface Modifications
B
12H HUASMC
Cells Internalising Spheres (%)
60
40
20
0
100
300
500
1000
Size (nm)
Negative
Neutral
PEGylated
PEGylated
Neutral
Negative
Surface Modifications

Figure 7

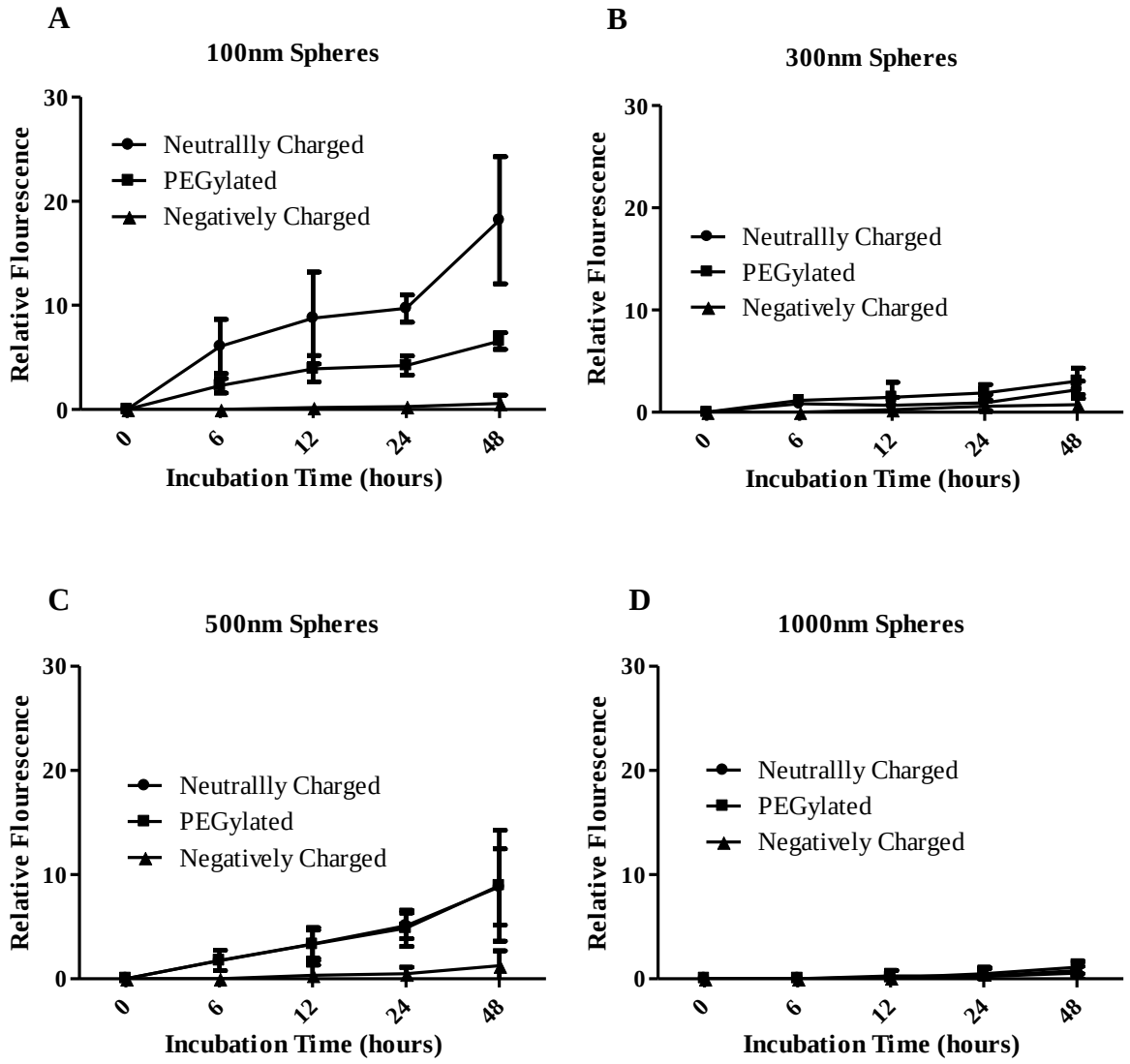
A
100nm Spheres
Relative Flourescence
Neutrallly Charged
PEGylated
Negatively Charged
Incubation Time (hours)
B
300nm Spheres
Relative Flourescence
Neutrallly Charged
PEGylated
Negatively Charged
Incubation Time (hours)
C
500nm Spheres
Relative Flourescence
Neutrallly Charged
PEGylated
Negatively Charged
Incubation Time (hours)
D
1000nm Spheres
Relative Flourescence
Neutrallly Charged
PEGylated
Negatively Charged
Incubation Time (hours)

Figure 8

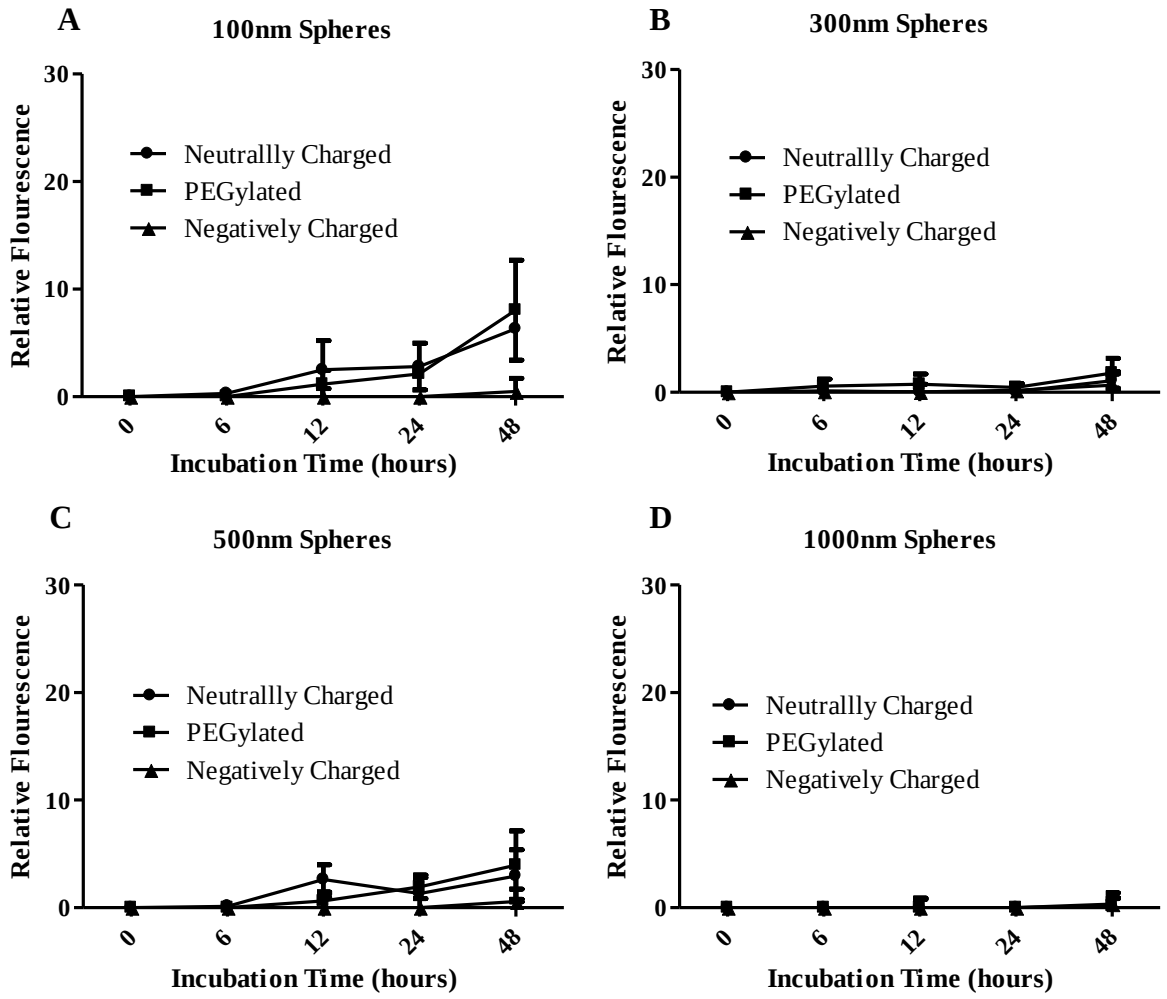
A
100nm Spheres
Relative Flourescence
30
20
10
0
Neutrallly Charged
PEGylated
Negatively Charged
0
6
12
24
48
Incubation Time (hours)
B
300nm Spheres
Relative Flourescence
30
20
10
0
Neutrallly Charged
PEGylated
Negatively Charged
0
6
12
24
48
Incubation Time (hours)
C
500nm Spheres
Relative Flourescence
30
20
10
0
Neutrallly Charged
PEGylated
Negatively Charged
0
6
12
24
48
Incubation Time (hours)
D
1000nm Spheres
Relative Flourescence
30
20
10
0
Neutrallly Charged
PEGylated
Negatively Charged
0
6
12
24
48
Incubation Time (hours)

Figure 9

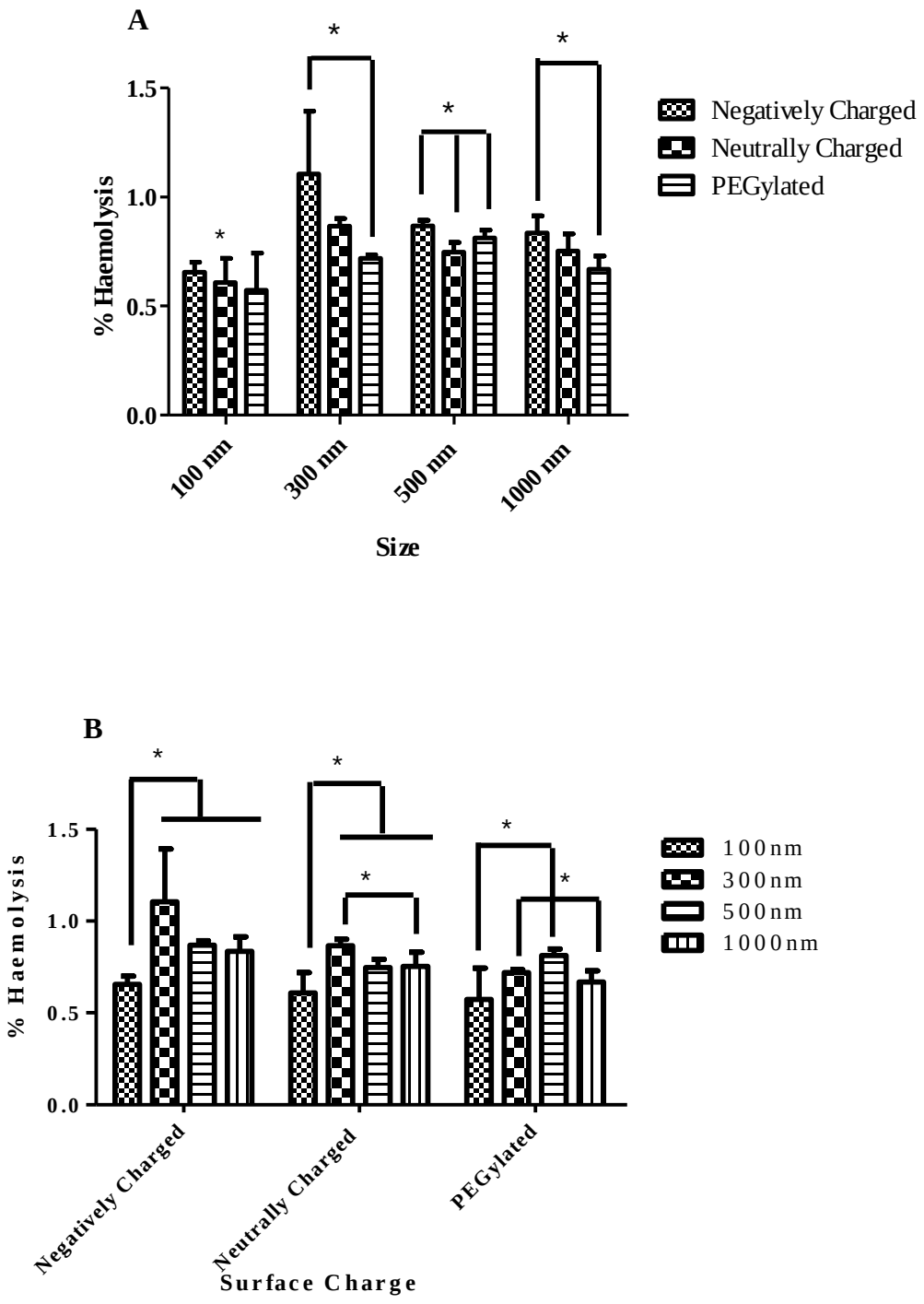
A
% Haemolysis
1.5
1.0
0.5
0.0
100 nm
300 nm
500 nm
1000 nm
Size
Negatively Charged
Neutrally Charged
PEGylated
B
% Haemolysis
1.5
1.0
0.5
0.0
Negatively Charged
Neutrally Charged
PEGylated
Surface Charge
100nm
300nm
500nm
1000nm

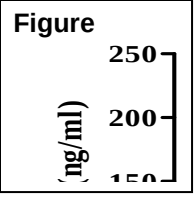
Figure
250
200
(ng/ml)

Figure 10

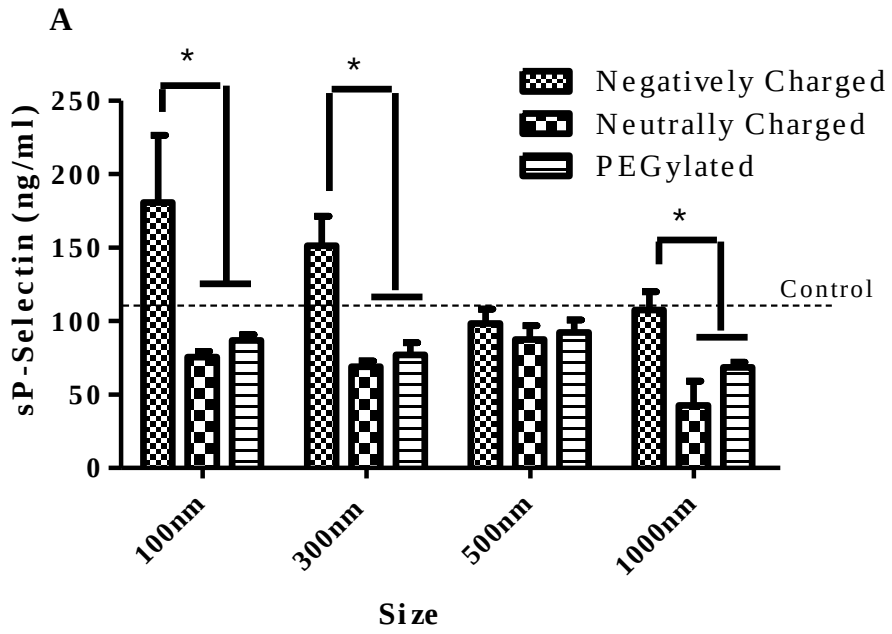
A
*
*
*
Negatively Charged
Neutrally Charged
PEGylated
Control
sP-Selectin (ng/ml)
250
200
150
100
50
0
100nm
300nm
500nm
1000nm
Size

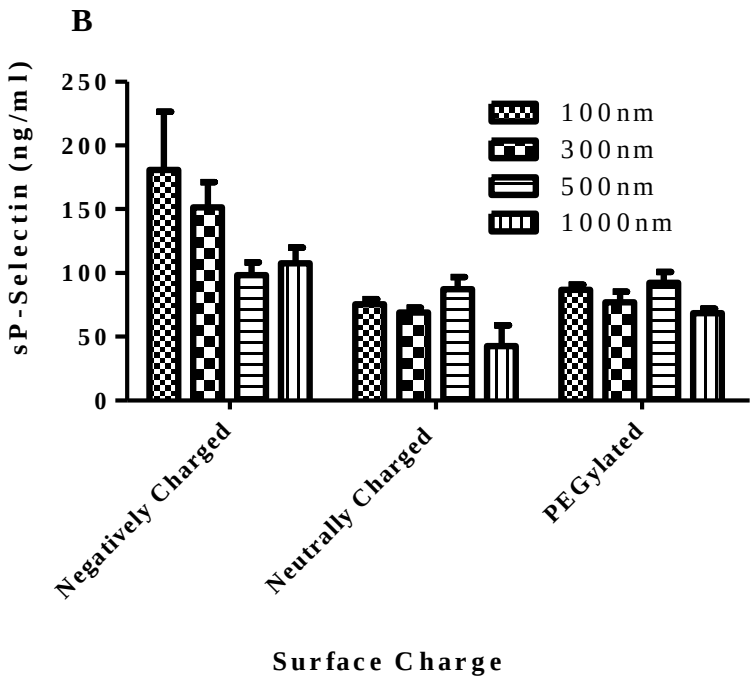
B
100nm
300nm
500nm
1000nm
sP-Selectin (ng/ml)
250
200
150
100
50
0
Negatively Charged
Neutrally Charged
PEGylated
Surface Charge

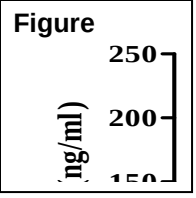
Figure
250
200
ng/ml)

Figure 11

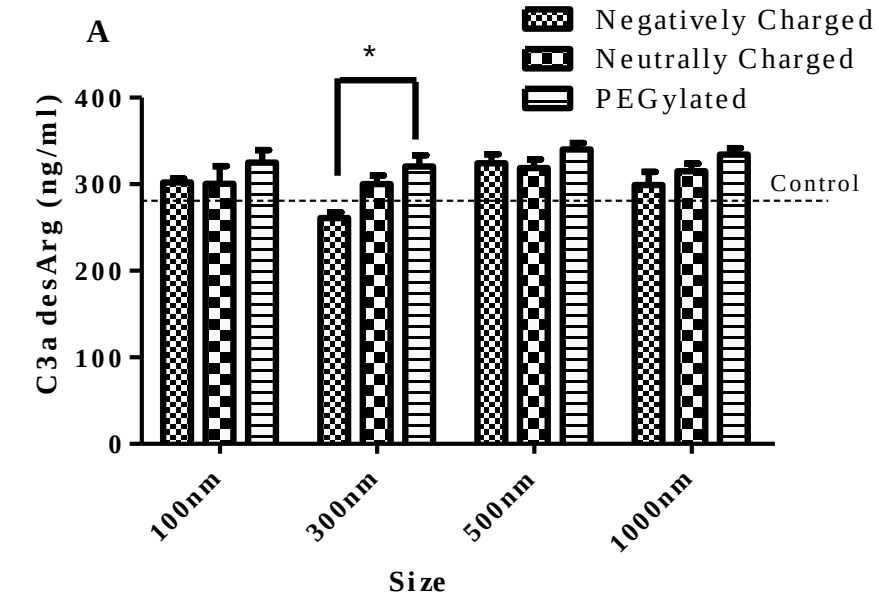
A
Negatively Charged
Neutrally Charged
PEGylated
*
Control
C3a desArg (ng/ml)
400
300
200
100
0
100nm
300nm
500nm
1000nm
Size

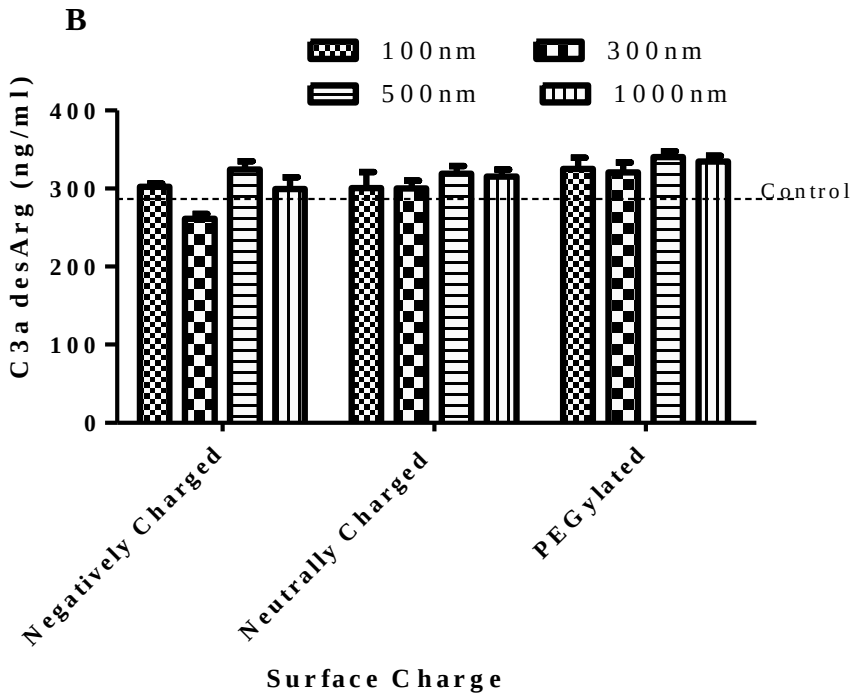
B
100nm
300nm
500nm
1000nm
Control
C3a desArg (ng/ml)
400
300
200
100
0
Negatively Charged
Neutrally Charged
PEGylated
Surface Charge

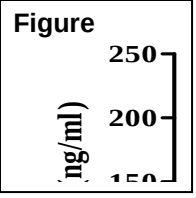
Figure
250
200
ng/ml)

Figure 12

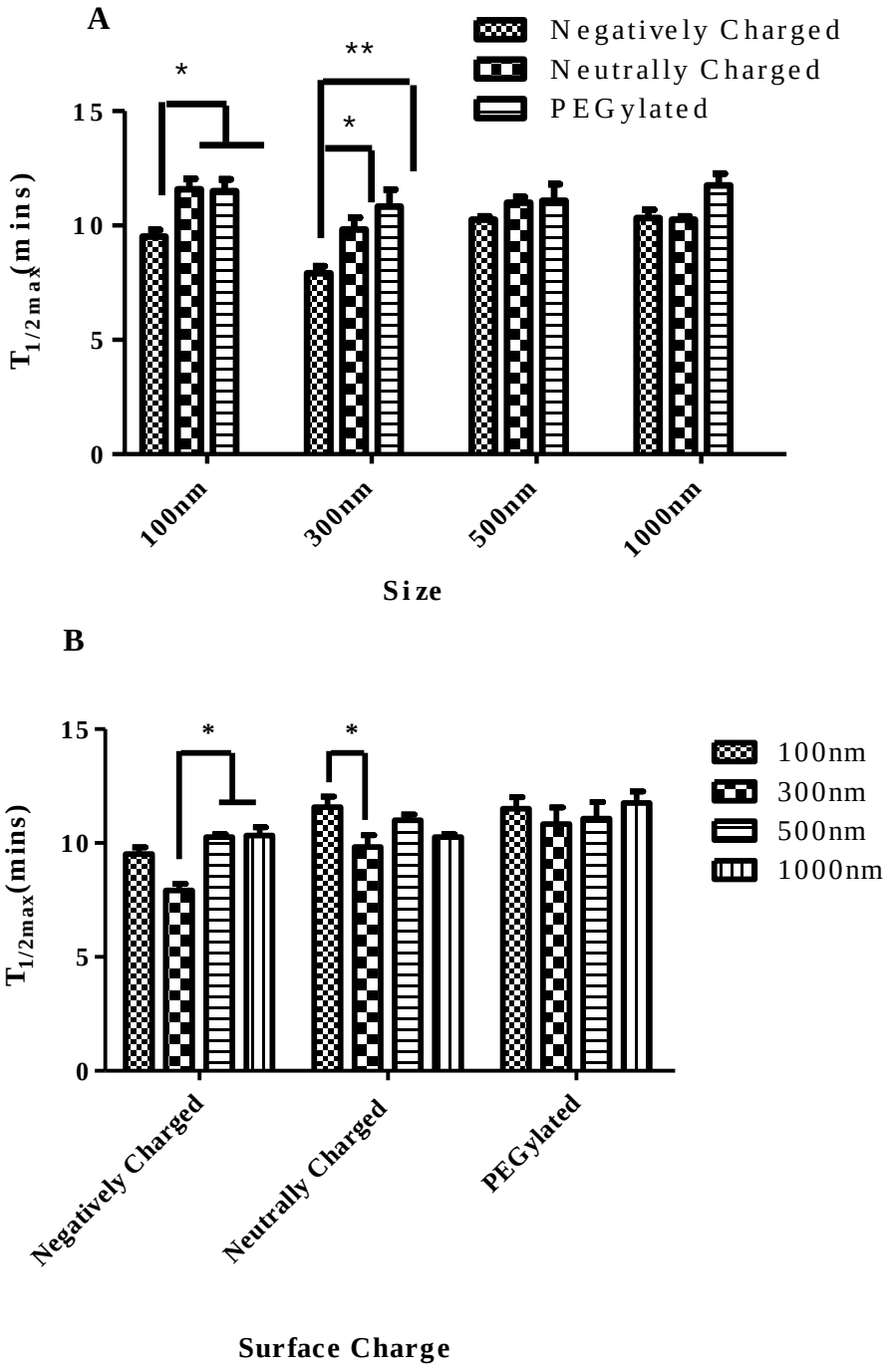
A
Negatively Charged
Neutrally Charged
PEGylated
*
**
*
15
10
5
0
T1/2max(mins)
100nm
300nm
500nm
1000nm
Size
B
*
*
15
10
5
0
T1/2max(mins)
100nm
300nm
500nm
1000nm
Negatively Charged
Neutrally Charged
PEGylated
Surface Charge

Figure

Supplementary Information

Results:

Cell Viability

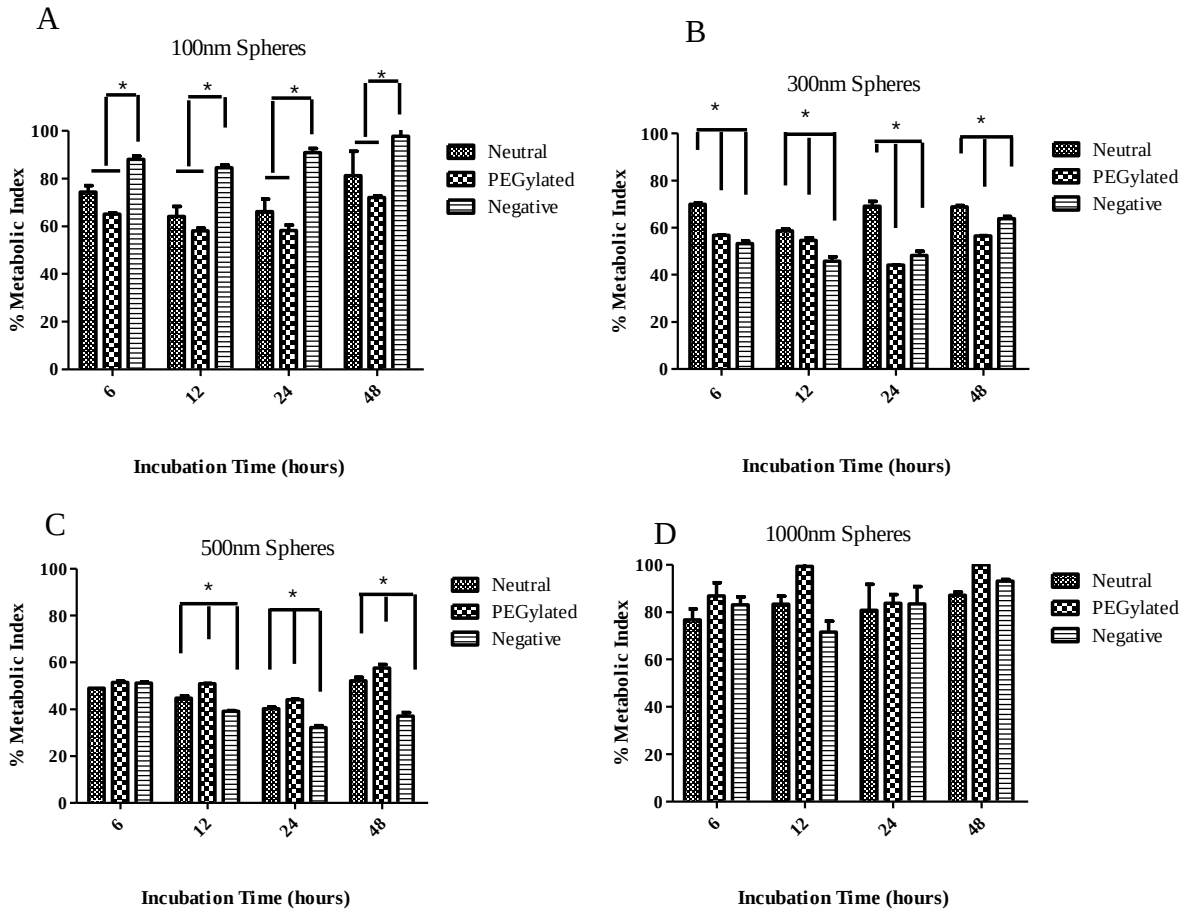

Figure 1: MTT assay showing percentage metabolic index of HUVECs at time points 6, 12, 24 and 48 hours. HUVECs were incubated with (A) 100nm, (B) 300nm, (C) 500nm and (D) 1000nm spheres. Data is represented as the mean ± standard deviation (n = 3). * indicates statistical significance ($p < 0.05$)

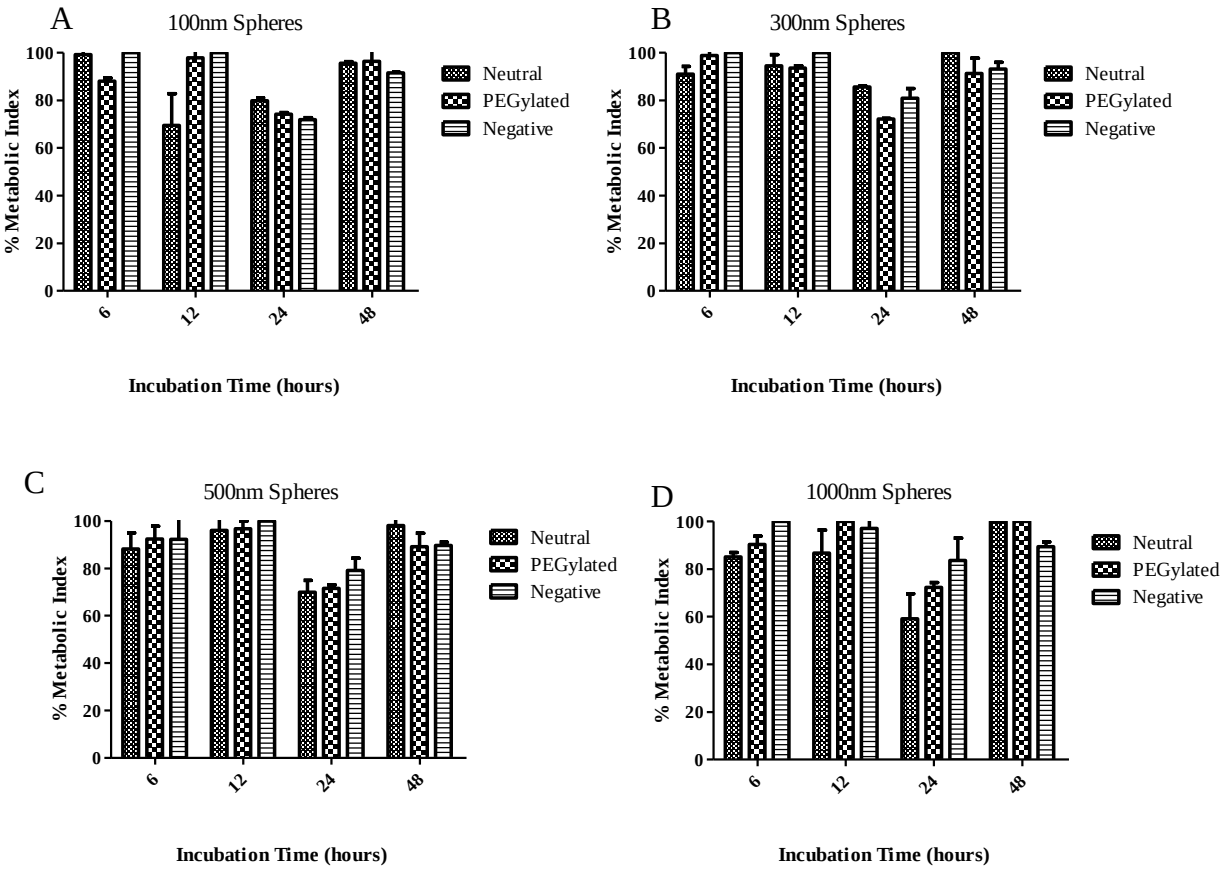

Figure 2: MTT assay showing percentage metabolic index of HUASMCs at time points 6, 12, 24 and 48 hours. HUASMCs were incubated with (A) 100nm, (B) 300nm, (C) 500nm and (D) 1000nm spheres. Data is represented as the mean ± standard deviation (n = 3). No statistically significant effect of surface functionalization was observed between spheres.

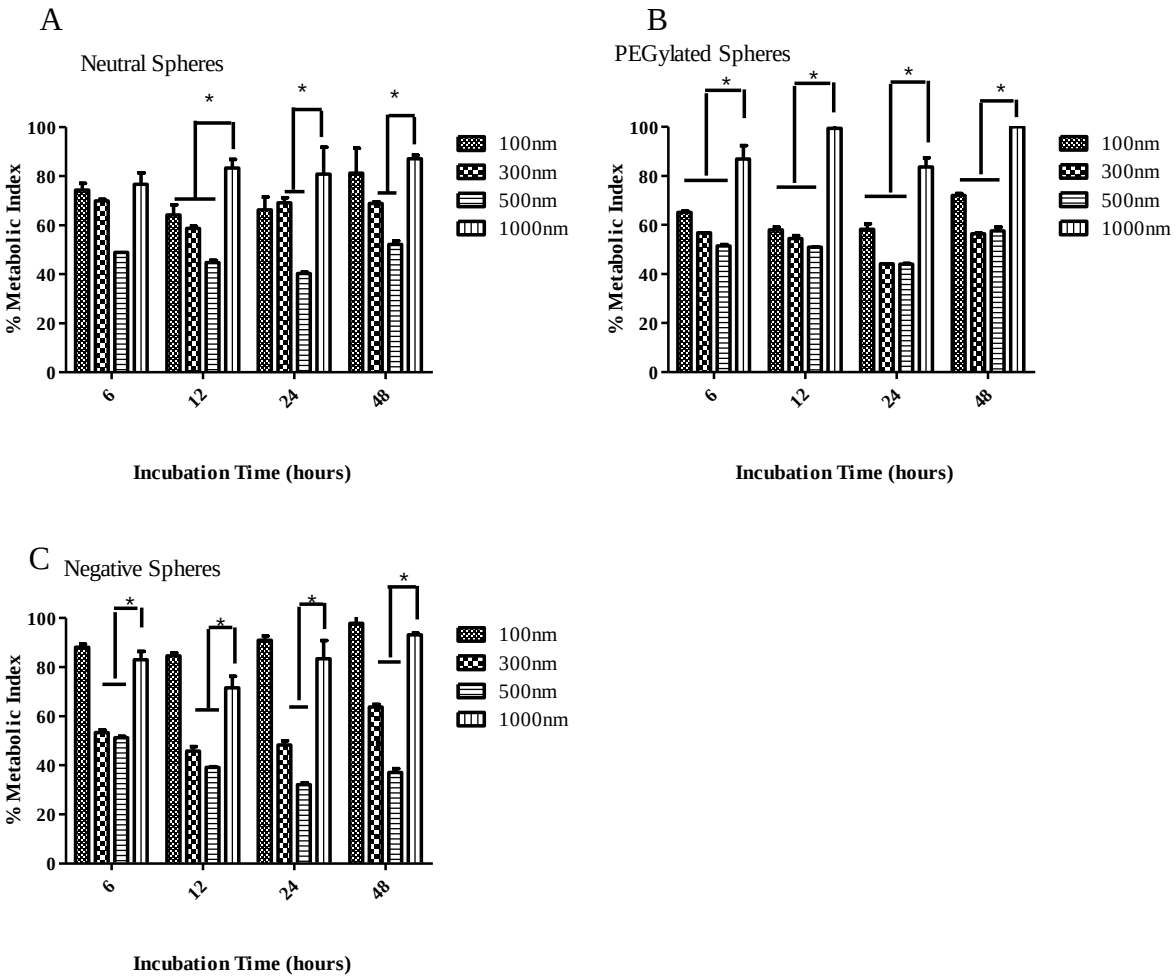

Figure 3: MTT assay showing percentage metabolic index of HUVECs at time points 6, 12, 24 and 48 hours. HUVECs were incubated with (A) Neutral, (B) PEGylated and (C) Negative spheres. Data is represented as the mean ± standard deviation (n = 3). * indicates statistical significance ($p < 0.05$)

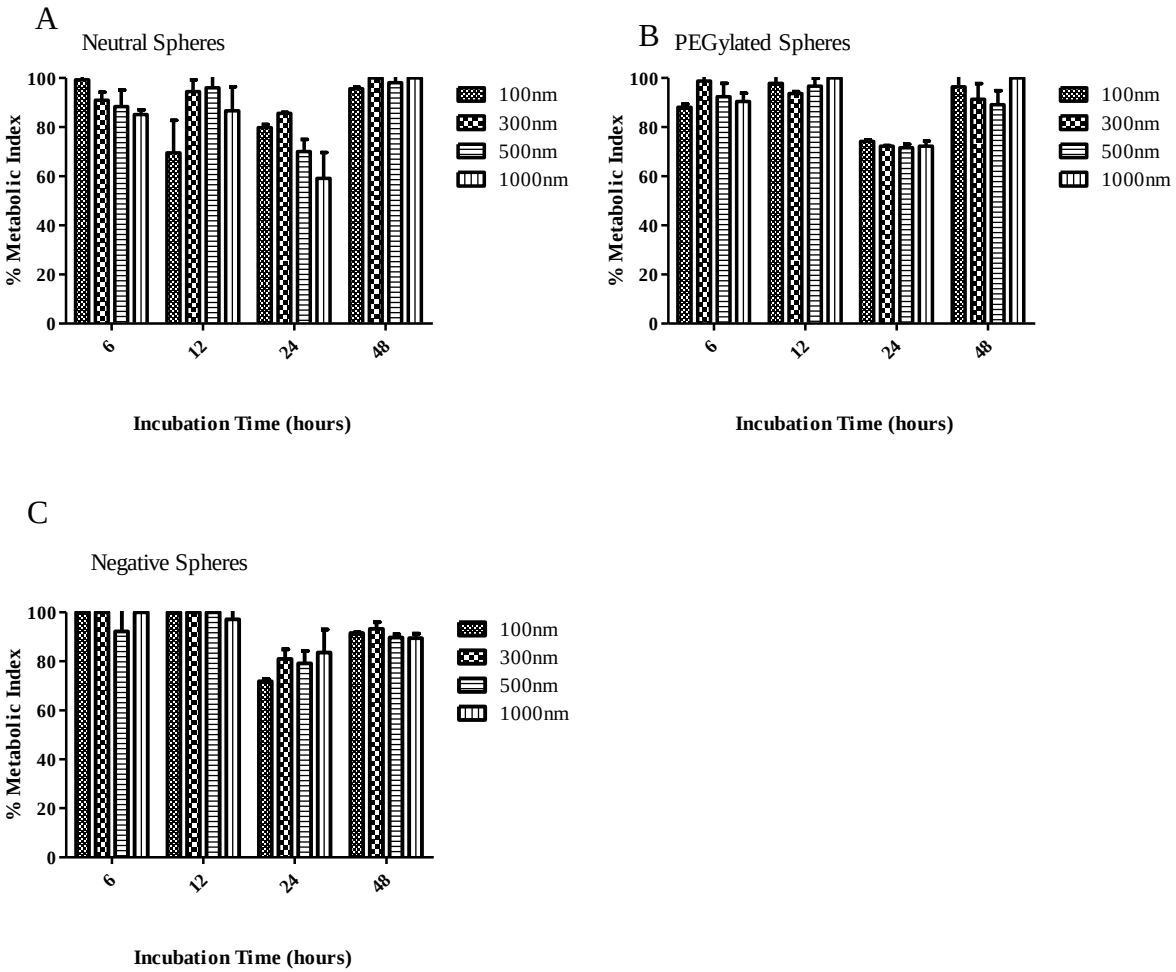

Figure 4: MTT assay showing percentage metabolic index of HUASMCs at time points 6, 12, 24 and 48 hours. HUASMCs were incubated with (A) Neutral, (B) PEGylated and (C) Negative spheres. Data is represented as the mean ± standard deviation (n = 3). No statistically significant effect of size was observed between spheres.